

Thesis for the Master's degree in chemistry

Jon Henriksen Austad

**Møller-Plesset theory
to second order for
the study of molecular
systems in finite
magnetic fields**

60 study points

DEPARTMENT OF CHEMISTRY

Faculty of mathematics and natural sciences

UNIVERSITY OF OSLO

May - 2013



Preface

I wish to thank my supervisors, professor Trygve U. Helgaker and Dr. Erik I. Tellgren, for their infinite patience when guiding me through this project. Especially Erik, whose responsibility it was to guide me through the process of understanding not only the algorithm to be implemented, but also the LONDON program itself. I also wish to thank Patrick Merlot, Kai K. Lange, Johannes Rekkedal, Vadimir Rybkin, Simen S. Reine, Stella Stopkowitz and Heike Fliegl for their support, patience, and willingness to help me whenever I had questions or needed help. A very special thanks goes to John C. Earles and Marianne H. Austad, whose red pens removed a vast number of misspelled words and grammatically questionable sentences. Without the collective aid of all these people, this project would not have been possible.

Abstract

London orbitals allows for non-perturbative treatment of magnetic fields. This can be used to explore how molecules behave in very strong finite magnetic fields, and also be used to probe complicated magnetic properties like hypermagnetizability without resorting to response theory. Classical MP2 and an atomic orbital based variant of MP2 with a Laplace transform ansatz were introduced to the LONDON program, and successfully used to perform different quantum chemical calculations entailing magnetic fields of finite size.

Contents

Preface	iii
Abstract	v
I Exordium	1
1 Introduction and Motivation	3
1.1 Computational chemistry	3
1.1.1 A different approach	3
1.1.2 A complicated endeavor	4
1.1.3 Methods, software and challenges	5
1.2 The aim of this master thesis	6
II Theory and Background	7
2 A brief look at quantum mechanics	9
2.1 The wave function	9
2.2 The Schrödinger equation	10
2.3 Spin	10
2.4 Operators	11
2.4.1 Bra-ket notation	11
2.4.2 Hermiticity	11
2.4.3 Second quantization	13
2.4.4 Approximations of the wave-function	14
2.5 The Rayleigh-Ritz variational principle	17
2.6 Size extensivity	18

3	Quantum chemistry in magnetic fields	19
3.1	Implications for quantum the mechanical formulation	19
3.2	Chemistry in strong magnetic fields	21
3.2.1	Strong and weak fields	22
3.3	Magnetic properties	23
3.3.1	Magnetizabilities	23
3.4	Some pitfalls when dealing with magnetic fields	25
4	London orbitals and gauge invariance	27
4.1	Introduction to orbital theory	27
4.2	Magnetic gauge and its implications	28
5	Quantum Chemical methods	33
5.1	Hartree-Fock Theory	33
5.2	Perturbative methods	35
5.2.1	Perturbation theory	35
5.2.2	Møller-Plesset perturbation theory (MPPT)	37
5.3	Two other methods worth mentioning	39
5.3.1	Configuration Interaction theory	39
5.3.2	Coupled cluster theory	40
III	Implementation and results	43
6	Implementation	45
6.1	Implementation of classical MP2	45
6.2	Implementation of Laplace-MP2	47
6.2.1	The Laplace transform ansatz	47
6.2.2	Implementing the Laplace-MP2 algorithm	47
6.2.3	Setting up the calculation and fitting	49
6.2.4	Integral screening	55
6.2.5	A small test case	55
6.2.6	Scaling	55
7	Results	61
7.1	Molecules in magnetic fields	61
7.1.1	Helium clusters	61
7.1.2	An example of paramagnetic stabilization	66
7.2	Magnetizabilities and hypermagnetizabilities	69

7.2.1	Magnetic properties of He ₂	70
7.2.2	Magnetic properties of water	70
7.2.3	London orbitals and basis set convergence	73
7.2.4	Order of polynomial fitting	74
7.2.5	An example of MP2 failing	75
IV	Discussion	79
8	Conclusion	81
8.1	About the implementation	81
8.1.1	MP2 in the CAS-type methods	81
8.1.2	Laplace MP2	81
8.2	Discussion of the results	82
8.2.1	Geometrical properties	83
8.2.2	Magnetic properties	83
8.2.3	Future systems to be explored	83
V	Appendix	89
A	Input data	91
A.1	Molecular geometries	91
A.1.1	Water	91
A.1.2	Water II	91

Part I
Exordium

Chapter 1

Introduction and Motivation

1.1 Computational chemistry

Chemistry is an old scientific discipline, and traces its roots back to the ancient alchemists. It remained a purely empirical discipline for centuries. Classical physics was the first branch of science to get a firm mathematical foundation, and therefore the first field where unknown systems could be predicted *a priori*. Since the nature of electrons and nuclei are inherently quantum mechanical, chemistry could not be treated in a fully theoretical manner until quantum mechanics was established. However, in the early years of quantum mechanics, only small systems like H_2 and helium atoms could be treated accurately. For larger systems this was still not feasible due to a lack of good methods and computational power. Resolving the first problem is an ongoing process that has given rise to a large variety of different many-body methods suited for specific purposes, and the latter was largely solved with the arrival of the electronic computer.¹

1.1.1 A different approach

Quantum chemistry today has become a popular tool in the toolbox of a modern chemist: when experimental results are in agreement with the radically different approach of quantum chemistry, then the observation has a very firm justification – two paths, one based on meticulous observations of what happens *as is*, and another that starts out in the very abstract realm of physical postulates and mathematical methodology.

¹Of course, more powerful machines are always in demand.

From a practical perspective, quantum chemistry may be used to screen experiments, remove large portions of unnecessary work, and of course, provide results when experimental data are not available. The latter is actually a quite common problem: some reactions require substances that are very difficult to deal with or highly dangerous, and some conditions are simply impossible to replicate in a lab. For example, one of the strongest continuous magnetic field produced in a lab to date has a magnitude of approximately 45T,² while certain stellar conditions may produce fields that are larger by several orders of magnitude. Hopefully, better magnets will be made in the future³ so that experiments and predictions may be compared, but as of yet, chemistry in strong magnetic fields remains a purely theoretical exercise. However, a molecule's response to a magnetic field depends, amongst other things, on its cross section area. Therefore, it is hypothesized that larger molecules will experience such effects at smaller fields, and thus let theory and experiment meet in a lab.

1.1.2 A complicated endeavor

Efficient numerical treatment of large electronic systems is difficult. This is partly due the so-called "curse of dimensionality": all electrons are described by three spatial coordinates and one spin coordinate. The dimensionality of the total system therefore becomes $4N$ where N is the number of electrons. Even a simple molecule like C_2H_5OH will therefore represent an 80-dimensional object, only counting the electrons. This is a quantum mechanical equivalent of the many-body problem that is often encountered in classical physics, which is a set of systems that in general does not have an analytical solution. Therefore, approximations must be made. However, with approximations come errors, and knowing the strengths and weaknesses of the methods involved is an important part of the trade. In computational chemistry we deal with a large family tree where all different levels of theory have their own branch. In this project, we will deal exclusively with *ab initio* computational chemistry methods. This family of methods are derived directly from quantum mechanical postulates. Other schemes, like molecular mechanics, are founded on classical physics.

²One of the strongest magnets in the world today resides at the the National High Magnetic Field Laboratory in the USA and can produce a field of 45T.

³This kind of reasoning is less pretentious than it may seem at first glance – after all, Peter Higgs predicted the existence of a certain boson back in 1964, a prediction that ultimately led to the construction of the Large Hadron Collider at CERN.

1.1.3 Methods, software and challenges

There are many methods and programs for solving quantum chemical problems. The purpose of the program will often reflect the choice of methods included and the manner in which they are implemented: a program constructed to solve a specific class of problems very fast (typical for commercial programs) will be inherently different to a program tailored towards more academic experimentation and modification. The DALTON program suite is an example of the latter, and sports a vast array of very different methods and can do anything from geometry optimization to response theory.⁴

Some systems are inherently more complicated to solve than others, and one family of problems that stands out as particularly difficult to deal with is magnetic fields.

Chemistry in magnetic fields and magnetic properties

The term “magnetic properties” is something most people will associate with classical ferromagnets, but all matter surrounding us has magnetic properties. All closed-shell systems are diamagnetic, and will as such be repelled slightly from magnetic fields. This effect is very weak, but is easily observable with the right equipment. Similarly, some materials are paramagnetic, and are attracted to magnetic fields.

In very strong magnetic fields, molecular systems can behave radically different. It should also be noted that there are a multitude of magnetic properties of bulk matter that are relatively unknown outside of certain academic circles, like anti-ferromagnetism, ferrimagnetism and parasitic ferromagnetism to mention a few [1].

How systems react to magnetic fields determine their magnetic properties, which are highly relevant – NMR shielding constants are one very notable example.

Magnetizabilities and especially hypermagnetizabilities have seen less attention [2, 3].

The London program

Quantum chemical calculations in strong magnetic fields is riddled with difficulties, and has as a consequence not seen very much attention. There are many ways to handle magnetic fields, but the most elegant and robust solution requires different atomic orbitals which are *non-perturbative* and *gauge origin invariant*. Normal quantum chemistry software cannot handle such orbitals as it again entails more general

⁴Response theory is a perturbative method for determining molecular properties in time-dependent potentials.

function and integral evaluations. This is a lot of work to implement. Hence, it has never been done – until LONDON [4].

The purpose of LONDON is to perform calculations on chemical systems in finite magnetic fields in a consistent and reliable manner, and the program was written from scratch with this in mind. The code is made to deal with the unexpected, and should be generalizable to meet the criteria of more or less any new and strange system. Therefore, generality is favored over numerical efficiency. This in turn means that many of the assumptions and “tricks” that almost everyone use to simplify their equations or speeding up their code may not be applicable. LONDON has support for both conventional Gaussian type orbitals and the gauge including London type orbitals. Most endeavors so far are based on perturbative approaches, which are known to behave erratically and unpredictably for strong magnetic fields. LONDON dispensed with this problem, but does not yet sport a full array of necessary methods.

1.2 The aim of this master thesis

This body of work consists of an implementation part and a calculation part. The implementation part introduces Møller-Plesset Perturbation Theory (MPPT) of second order (MP2) to LONDON. This method was absent, and it fills an important role: MP2 can be used to calculate correlation energy in LONDON, and it is much faster than the FCI method which was already present. It is not quite as accurate, but since FCI calculations with a reasonable basis set can only include a hand full of atoms *at most*⁵, an MP2 implementation is highly advantageous. In LONDON, speed was sacrificed for generality, and complex valued orbitals make several calculations intrinsically slower. For these reasons, faster methods like MP2 are essential. MP2 was introduced in two variants: “classical” MP2 and atomic-orbital MP2 with a Laplace transformation ansatz. The details will be dealt with in depth in chapter 5. Using these methods to calculate different properties of some molecules in various magnetic fields comprise the second part of the project. The methods were used to predict quantum chemical properties in some small molecules.

⁵Indeed, the LONDON implementation cannot go much beyond four electrons. Other implementations that are more optimized can do a few more, but the FCI method is still restricted to very small molecules. Larger molecules can be treated by FCI with very small basis sets, but the results then obtained are largely useless.

Part II
Theory and Background

Chapter 2

A brief look at quantum mechanics

Scientists have always sought a complete theory that may be used to describe *all* physical phenomena. Classical physics can be used for a startling number of real problems, but it breaks down when things either move very fast or are very small. For these two cases, we have the general theory of relativity and quantum mechanics. They may of course be combined, but quantum electrodynamics is beyond the scope of this thesis, and we shall limit our attention to “classical” quantum mechanics. Quantum mechanics is inherently non-intuitive, but consistent experimentation over the last hundred years has revealed it to be one of the sturdiest and most powerful theories available [5]. Atomic units are assumed for the entirety of this thesis unless otherwise specified.

2.1 The wave function

In the absence of a magnetic field, the quantum mechanical wave-function Ψ contains all information about the system it describes.¹ The wave-function rarely has a closed form expression; only for the simplest systems is it even known. Also, while all observables by necessity are *real*, the wave-function itself is frequently *complex*. A large part of quantum mechanics is about the noble art of approximating the wave-function in a sensible way.

¹Indeed, *all* information that can be experimentally measured. What really constitutes a measurement, however, is a question best left to the philosophers.

2.2 The Schrödinger equation

The Schrödinger equation is perhaps the most important equation in the entire field of quantum mechanics. The time-dependent non-relativistic one-particle variant is

$$\left[-\frac{1}{2}\nabla^2 + \hat{\mathcal{V}} \right] \Psi(\mathbf{x}, t) = i\hbar \frac{\partial}{\partial t} \Psi(\mathbf{x}, t) \quad (2.1)$$

where $\hat{\mathcal{V}}$ is a possibly time-dependent, possibly position dependent potential. The time-independent equation is

$$\left[-\frac{1}{2}\nabla^2 + \hat{\mathcal{V}} \right] \Psi(\mathbf{x}) = E\Psi(\mathbf{x}) \quad (2.2)$$

where E is the energy of the system. These equations can be expanded to match a multi-particle system. Then, the kinetic part becomes a simple summation of terms, but the interactions between the electrons are complicated as all charged particles depend on each other simultaneously. The time-dependent Schrödinger equation is not relevant in this thesis.

2.3 Spin

Despite the name, spin is a purely quantum mechanical property. It is also an *intrinsic property*, just like mass, and all particles have spin of either integer value (bosons) or half-integer value (fermions). The associated quantum number is labeled s . Electrons have spin $\pm\frac{1}{2}$. It is also a kind of angular momentum. Quantum mechanics operates with two varieties: one is *orbital angular momentum* which describes a curved trajectory of a particle and corresponds to the concept of angular momentum in classical physics. The other is spin angular momentum.

Half-integer spin imposes restrictions. The most important is that a wave-function must be anti-symmetrical when two particles are interchanged. This is a consequence of the Pauli principle, which states that two identical fermions cannot possess the same set of quantum numbers.

Often, an electronic wave-function is described as a linear combination of one-electron functions. These functions contain coordinates describing the position of the orbital in space, and on spin coordinate describing the spin value. Such a one-particle state is called a *spinor*.

2.4 Operators

A mathematical *operator* is to a function what a function is to a variable. Differentiation is one example of an operator. Operators are essential in quantum mechanics as all observables are represented by operators. One neat thing about operators is that they can all be represented as matrices, which is very useful when doing computational science. Operators are associated with eigenfunctions (or eigenvectors in the matrix regime) and eigenvalues. The eigenvalues of a quantum mechanical operator represent an observable, whereas the eigenfunctions are typically the wave-function or some approximate variant thereof.

2.4.1 Bra-ket notation

The bra/ket-notation is a convenient notation when working with operators. A quantum state is described by a ket-vector $|p\rangle$. The $\langle p|$ -vector is the hermitian conjugate, so that for two states p and q

$$\langle p|q\rangle = \delta_{pq} \quad (2.3)$$

if the states are part of an orthonormal set. An expectation value of some operator \hat{O} is defined as

$$\langle \Psi | \hat{O} | \Psi \rangle \equiv \int \Psi(\mathbf{x})^* \hat{O} \Psi(\mathbf{x}) d\mathbf{x} \quad (2.4)$$

Where the Ψ is an eigenvector of \hat{O} .

2.4.2 Hermiticity

An operator is said to be *hermitian* if it is equal to its own *adjoint*:

$$\hat{O} = \hat{O}^\dagger \equiv (\mathbf{O}^*)^T \quad (2.5)$$

Of course, an operator is not the same as a matrix, and so it may seem inaccurate to claim that an operator can equal its own complex transpose. However, if the wave-function (or our approximation thereof) is represented as a vector, then the operator can be represented as a matrix. The operator's effect on a wave-function is then described as a matrix multiplication, which from a numerical perspective is very efficient. These mathematical objects also have many powerful properties, one of them being that

$$\left(\hat{O}_1 \hat{O}_2 |f\rangle \right)^\dagger = \langle f | \hat{O}_2 \hat{O}_1 \quad (2.6)$$

If an observable represented by a hermitian operator \hat{O} is measured, then the possible measured values are eigenvalues of \hat{O} . Since the operator in question is hermitian, the eigenvalues must be real by definition. The most important observable by far is energy, which is the eigenvalue of the *Hamiltonian operator* $\hat{\mathcal{H}}$.

The Hamiltonian

We define the Hamiltonian operator $\hat{\mathcal{H}}$ so that

$$\hat{\mathcal{H}}\Psi(\mathbf{x}) = E\Psi(\mathbf{x}) \quad (2.7)$$

which is a convenient way of writing the time-independent Schrödinger equation. The complete Hamiltonian for a many-particle scenario takes this form:

$$\hat{\mathcal{H}} = \underbrace{-\frac{1}{2} \sum_i \nabla_i^2 - \frac{1}{2} \sum_I \frac{\nabla_I^2}{M_I}}_{\text{Kinetic energy}} + \underbrace{\sum_{i<j} \frac{1}{\|\mathbf{r}_i - \mathbf{r}_j\|}}_{\text{Coulomb repulsion}} + \underbrace{\sum_{I<J} \frac{Z_I Z_J}{|\mathbf{r}_I - \mathbf{r}_J|}}_{\text{Coulomb attraction}} - \underbrace{\sum_{i,I} \frac{Z_I}{|\mathbf{r}_i - \mathbf{r}_I|}}_{\text{Coulomb attraction}} + \underbrace{\hat{\mathcal{V}}}_{\text{“Rest”}} \quad (2.8)$$

Upper and lower case indices refer to nuclei and electrons, respectively. $\hat{\mathcal{V}}$ is the potential, in this case “the rest” – whatever field etc. is not already included. Often, $\hat{\mathcal{H}}$ is split into a kinetic part and the Coulomb interactions are treated as a part of $\hat{\mathcal{V}}$. In electronic structure theory, we usually deal with a simplified Hamiltonian;

$$\hat{\mathcal{H}} = \underbrace{-\frac{1}{2} \sum_i \nabla_i^2}_{\hat{\tau}} + \underbrace{\sum_{i<j} \frac{1}{r_{ij}}}_{g_{ij}} - \underbrace{\sum_{i,I} \frac{Z_I}{r_{iI}}}_{\hat{\mathcal{V}}_{\text{ne}}} + \sum_{I<J} \frac{Z_I Z_J}{r_{IJ}} + \underbrace{\hat{\mathcal{V}}}_{\text{“Rest”}} \quad (2.9)$$

where the nuclei-nuclei parts are removed. These are instead treated “classically” as per the *Born-Oppenheimer approximation* (BO). This greatly reduces the dimensionality of the system to be calculated.

The Born-Oppenheimer approximation

A proton has more than 1800 times the mass of an electron. Therefore, the nucleus may be said to be relatively stationary compared with an electron, with the consequence that the electrons will redistribute themselves with any new configuration of the nuclei almost instantaneously. If we say that the nuclei actually *are* stationary, we

can invoke the BO and freeze out the electron-nuclei interactions. Mathematically, we split the wave-function into two parts:

$$\psi(\mathbf{r}, \mathbf{R}) \approx \psi_e(\mathbf{r}; \mathbf{R}) \chi(\mathbf{R}) \quad (2.10)$$

where \mathbf{R} is the coordinates of the nuclei and \mathbf{r} the coordinates of the electrons. The electronic wave-function ψ_e depends only parametrically on the coordinates of the nuclei. The function χ does not have the electrons as a parameter at all; the BO assumes that the nuclei are not affected by the electrons. This assumption breaks down in the case of highly excited rotational and vibrational states [6], but that is beyond the scope of this thesis.

2.4.3 Second quantization

Second quantization provides a useful notation for describing the methods used in quantum chemistry. An important concept is the *Fermi level*. Whether we have a molecule or an atom, we do have a set of orbitals that the electrons can occupy. These orbitals are lying at different energy levels. The Fermi level is a hypothetical level lying immediately between highest occupied and lowest un-occupied orbital in the ground state. The ground state must not be confused with the true vacuum state $|0\rangle$, which is a state devoid of particles. A common convention, which will be adopted here, is to denote particle states above the Fermi level by the indices $abc\dots$, hole states below as $ijk\dots$, and arbitrary levels as $pqr\dots$. Central to this notation is the creation and annihilation operators \hat{a}_p^\dagger and \hat{a}_p . The creation operator will summon a particle into the wave-function, the annihilation operator will banish it (or create a hole, depending on how one chooses to see it).

$$\begin{aligned} \hat{a}_p^\dagger |0\rangle &= |p\rangle \\ \hat{a}_p |p\rangle &= |0\rangle \end{aligned}$$

These operators are not hermitian, but they do have an interesting anti-commutation relationship:

$$\begin{aligned} \{\hat{a}_p, \hat{a}_q\} &= \{\hat{a}_p^\dagger, \hat{a}_q^\dagger\} = 0 \\ \{\hat{a}_p, \hat{a}_q^\dagger\} &= \delta_{pq} \end{aligned}$$

The true vacuum state $|0\rangle$ is not very useful, and so the state where all particles fill up the lowest lying orbitals from bottom up is assumed to be the ground state. All excitations must then consist of n holes under the Fermi level and n particles

above. A one-particle-one-hole excitation gets the short form 1p1h and so on. In bra/ket-notation, the 1p1h and 2p2h and n pnh becomes

$$\hat{a}_a^\dagger \hat{a}_i |\Phi_0\rangle = |\Phi_i^a\rangle \quad (2.11)$$

$$\hat{a}_a^\dagger \hat{a}_b^\dagger \hat{a}_i \hat{a}_j |\Phi_0\rangle = |\Phi_{ij}^{ab}\rangle \quad (2.12)$$

$$\prod_{ai} \hat{a}_a^\dagger \hat{a}_i |\Phi_0\rangle = |\Phi_{ijk\dots}^{abc\dots}\rangle \quad (2.13)$$

A general excited state with an unspecified number of excitations involved is denoted $|\Phi_H^P\rangle$. Some rules are

$$\hat{a}_i |0\rangle = 0$$

$$\hat{a}_a^\dagger |a\rangle = 0$$

which holds true for any state where said hole or particle is already present. Second quantization is general enough to handle systems of varying number of particles and it is therefore possible to change the total number of particles in a wave-function, even though this is unphysical. Therefore, rigorous book keeping is essential.

2.4.4 Approximations of the wave-function

We can have exact wave-functions only for a small set of very simple systems. It is therefore necessary to find a sensible approximation. One way is to write the total wave-function as a product of one-electron functions. Normally, a *molecular orbital* (MO) is written as a linear combination of *atomic orbitals* (AO). The MOs are orthonormal, but the AOs are not. The AOs are extracted from a basis set and are just a list of coefficients for one kind of function. The most common by far (and the only one which is used within the scope of this work) are Gaussian type functions.

Given one-electron states ϕ_k , this seems a reasonable way to make a many-particle wave-function;

$$\Pi(x_1, x_2, \dots, x_N) = \prod_{i=1}^N \phi_i(x_i) \quad (2.14)$$

however, this wave-function does not satisfy the Pauli principle. The Slater determinant (SD) is a better solution:

$$\Psi_{\text{SD}}(x_1, x_2, \dots, x_N) = \frac{1}{\sqrt{N!}} \begin{vmatrix} \phi_1(x_1) & \phi_1(x_2) & \dots & \phi_1(x_N) \\ \phi_2(x_1) & \phi_2(x_2) & \dots & \phi_2(x_N) \\ \vdots & \vdots & \ddots & \vdots \\ \phi_N(x_1) & \phi_N(x_2) & \dots & \phi_N(x_N) \end{vmatrix} \quad (2.15)$$

where each ϕ_k is a spinor. Typically, we use MOs, but AOs can also be used. The SD can be written more concisely

$$\Psi(x_1, x_2, \dots, x_N) = \frac{1}{\sqrt{N!}} \sum_p (-1)^p P \prod_i \phi_i(i) = \hat{\mathcal{A}} \prod_i \phi_i(i) = \hat{\mathcal{A}} \Pi \quad (2.16)$$

where P is the permutation operator and p is the number of columns to be interchanged. The operator $\hat{\mathcal{A}}$ is the *anti-symmetrization operator*, which sums over all sets of all possible permutations. This operator is hermitian and commutes with any observable $\hat{\mathcal{O}}$ – it must, because a permutation in the Slater determinant cannot change the eigenvalues of the operators. Therefore, it has some interesting properties;

$$\begin{aligned} \hat{\mathcal{A}}\hat{\mathcal{A}} &= \sqrt{N!}\hat{\mathcal{A}} \\ [\hat{\mathcal{A}}, \hat{\mathcal{H}}] &= 0 \end{aligned}$$

A single Slater determinant cannot be used for accurate description of a system: many phenomena cannot be described at all without 2p2h-excitations. Electron correlation is one notable example.

The energy of a Slater determinant

If we recall the Hamiltonian from equation (2.8) and apply it on the Slater determinant, we see immediately that the nuclei-nuclei parts becomes a constant V_{nn} – the Slater determinant is a purely electronic entity. That leaves us with the kinetic part $\hat{\mathcal{T}}$, the Coulomb attraction, the Coulomb repulsion and the remaining potential $\hat{\mathcal{V}}$. This latter part will be ignored for the time being. The remaining entities can be organized in terms of number of electron interactions; $\hat{\mathcal{T}}$ and the attraction between nuclei and electrons are sums of one-electron operators, while the Coulomb repulsion constitutes a sum over all pairs of electrons.² We can now define an electronic Hamiltonian $\hat{\mathcal{H}}_e$:

$$\sum_i \hat{h}_i = \hat{\mathcal{T}} + \hat{\mathcal{V}}_{\text{ne}} \quad (2.17)$$

$$\hat{\mathcal{H}}_e = \sum_i \hat{h}_i + \sum_{i < j} \hat{g}_{ij} + V_{\text{nn}} \quad (2.18)$$

$$E[\Psi_{\text{SD}}] = \langle \Psi_{\text{SD}} | \hat{\mathcal{H}}_e | \Psi_{\text{SD}} \rangle \quad (2.19)$$

²Fortunately, we don't need to deal with three-body operators, but in certain fields of sub-atomic physics, such forces are relevant.

The expectation values of the one-electron parts are nothing but a sum of non-interacting orbital energies

$$\langle \phi_i | \phi_j \rangle = \delta_{ij} \quad (2.20)$$

$$\langle \phi_i | \hat{h}_i | \phi_i \rangle = h_{ii} \quad (2.21)$$

$$\Rightarrow \langle \Pi | \hat{\mathcal{T}} + \hat{\mathcal{V}}_{\text{ne}} | \Pi \rangle = \sum_i \langle \phi_i | \hat{h}_i | \phi_i \rangle \quad (2.22)$$

Therefore, the only thing left that needs to be evaluated is the two-body contributions. It is convenient to rewrite equation (2.16) so that we get

$$\langle \Psi_{\text{SD}} | \hat{\mathcal{V}}_{\text{ee}} | \Psi_{\text{SD}} \rangle = \langle \hat{\mathcal{A}}\Pi | \hat{\mathcal{V}}_{\text{ee}} | \hat{\mathcal{A}}\Pi \rangle \quad (2.23)$$

$$= \sum_p (-1)^p \langle \Pi | \hat{\mathcal{V}}_{\text{ee}} | \mathbf{P}\Pi \rangle \quad (2.24)$$

$$(2.25)$$

Only the identity and two-electron permutations can contribute according to Wicks theorem. The operator g_{ij} only acts on MOs i and j (for reasons of readability, we define $\phi_k(k) = k$), such that

$$\langle \Pi | g_{ij} | \Pi \rangle = \langle 1 | 1 \rangle \langle 2 | 2 \rangle \dots \langle ij | g_{ij} | ij \rangle \dots \langle N | N \rangle \quad (2.26)$$

This is the case for the identity operator; i.e. that $P = \mathbb{I}$. For other permutations, we see that the integral is zero unless the indices of P and \mathbf{g} matches. We get two possibilities:

$$\langle \Pi | g_{ij} | \mathbb{I}\Pi \rangle = \langle \phi_i(i)\phi_j(j) | g_{ij} | \phi_i(i)\phi_j(j) \rangle = J_{ij} \quad (2.27)$$

$$\langle \Pi | g_{ij} | P_{ij}\Pi \rangle = \langle \phi_i(i)\phi_j(j) | g_{ij} | \phi_i(j)\phi_j(i) \rangle = K_{ij} \quad (2.28)$$

where $\hat{\mathcal{J}}$ and $\hat{\mathcal{K}}$ are the *Coulomb* and *exchange* operators. The former is analogous to classical electrostatic repulsion, the latter is purely quantum mechanical in nature. A rewriting of equation (2.19) now yields

$$E[\Psi_{\text{SD}}] = \sum_i h_{ii} + \frac{1}{2} \sum_{ij} (J_{ij} - K_{ij}) + V_{\text{nn}} \quad (2.29)$$

Where the minus sign of K_{ij} is caused by the permutation performed on the ket-vector, and the factor $\frac{1}{2}$ is an offset to the free summation over both i and j . The next step is now to define the molecular orbitals. This will be dealt with in section 4.1.

2.5 The Rayleigh-Ritz variational principle

Any approximated wave-function ϕ that occupies Hilbert space must by necessity be a linear combination of the eigenstates of $\hat{\mathcal{H}}$. Therefore

$$\phi = \sum_n c_n \psi_n$$

Since the ground state energy by definition is

$$E_0 = \langle \psi_0 | \hat{\mathcal{H}} | \psi_0 \rangle$$

it follows that

$$\langle \phi | \hat{\mathcal{H}} | \phi \rangle \geq E_0 \quad \forall \phi$$

As is implied by the name, the variational method employs a set of variational parameters $\boldsymbol{\lambda} = \{\lambda_1, \lambda_2, \dots, \lambda_N\}$ so that

$$\langle \phi(\boldsymbol{\lambda}) | \hat{\mathcal{H}} | \phi(\boldsymbol{\lambda}) \rangle = E(\boldsymbol{\lambda})$$

The optimal set of parameters is therefore a question of derivation with respect to all parameters. Of course, if the wave-function is optimized with respect to energy, then there is no *a priori* reason to assume it is also optimized for other variables. However, in practice, a very precise calculation of energy can be used reliably for other values as well. The beauty of the variational approach lies in the fact that while it may not necessarily provide the exact energy of the system, it will provide an upper bound. One way to test if a set of variational parameters $\boldsymbol{\lambda}$ is optimal is to look at the derivatives of energy with respect to these parameters. If

$$\begin{aligned} \frac{dE_{\boldsymbol{\lambda}}}{d\boldsymbol{\lambda}} &= 0 \\ \frac{d^2 E_{\boldsymbol{\lambda}}}{d\boldsymbol{\lambda}^2} &\geq 0 \end{aligned}$$

holds, then that set provides a true minimum. Perturbative methods are unfortunately *not* variational. However, the principle is important for understanding Hartree-Fock theory.

2.6 Size extensivity

If a system consists of N non-interacting parts, then there are two obvious ways of treating it. One is to describe everything by a single wave-function, the other is to treat the N subsystems individually. Since the systems are non-interacting, any variant of the Hamiltonian should provide the same end-result. This property is called *size-extensivity* [7]. One example where the importance of such behavior is essential is chemical dissociation reactions like $AB \rightarrow A + B$. As the fragments move apart, the total energy of the system should be comparable with the individual energies:

$$\begin{aligned}\Psi_{AB} &= \Psi_A \Psi_B \\ \hat{\mathcal{H}}\Psi_{AB} &= \left(\hat{\mathcal{H}}_A + \hat{\mathcal{H}}_B\right) \Psi_A \Psi_B \\ \Rightarrow E_{AB} &= E_A + E_B\end{aligned}$$

In other words, the wave-functions are separable, and the Hamiltonian for each subsystem does not affect other parts of it. If $E_{AB} \neq E_A + E_B$, it is difficult to evaluate the quality of the results.

Size extensivity holds true for all exact representations of the wave-function. However, there is no mathematical necessity that all approximations must behave in this manner, even though it is highly desirable.

In this project, we deal with a perturbed wave-function, and therefore it is inherently size-extensive.

Chapter 3

Quantum chemistry in magnetic fields

Quantum mechanics allows for great generality, but in practice, we usually impose a number of restrictions and assumptions in order to simplify our calculations. For example, in the presence of only electrostatic potentials, the system is symmetric under time-reversal. The quantum mechanical time-reversal operation has two components: one that affects only spin, and one that is essentially complex conjugation[8]. It is therefore possible in this case to choose real wave-functions and energy eigenstates. A magnetic field breaks this symmetry. Therefore, many common expressions are slightly different in the presence of a magnetic field.

There are two ways in which magnetic fields are interesting from a chemists point of view. One is how a chemical system behaves in a magnetic field. The other is to determine magnetic properties of molecules.

One “standard” atomic unit of a magnetic field translates to 2.35 kT in SI units. The fields employed in this thesis range from about 10^{-5} a.u. to 2 a.u.

3.1 Implications for quantum the mechanical formulation

For this thesis, the most immediate difference is the distinction between different types of momenta. In the absence of a magnetic field, we need only concern ourselves with the canonical momentum operator $\hat{\mathbf{p}}$. The concept of momentum is analogous

to classical physics where

$$\mathbf{p} = m\mathbf{v} \quad (3.1)$$

$$E_K = \frac{1}{2}mv^2 = \frac{1}{2m}p^2 \quad (3.2)$$

describes the relationship between velocity, momentum and kinetic energy. In quantum mechanics, the expression is usually written differently, but the meaning is very much the same (SI units added for illustrative purposes):

$$\hat{\mathbf{p}} = -i\hbar\nabla \quad (3.3)$$

$$\frac{1}{2m}\hat{p}^2 = -\frac{\hbar^2}{2m}\nabla^2 \quad (3.4)$$

In order to add magnetic fields to quantum mechanics, a more general definition of momentum is required. Therefore, we introduce the a new momentum operator $\hat{\boldsymbol{\pi}}$:

$$\hat{\boldsymbol{\pi}} = \hat{\mathbf{p}} - q\mathbf{A} \quad (3.5)$$

where q is the charge of the particle (which is -1 for an electron when we use atomic units) and \mathbf{A} is the *magnetic vector potential*. This is defined by

$$\mathbf{A} = \frac{1}{2}\mathbf{B} \times (\mathbf{r} - \mathbf{g}) \quad (3.6)$$

where \mathbf{g} is the gauge origin. It must be emphasized that \mathbf{A} satisfies the homogeneous pair of Maxwell's equations:

$$\nabla \cdot \mathbf{B} = 0 \quad (3.7)$$

$$\nabla \times \mathbf{E} + \frac{\partial \mathbf{B}}{\partial t} = 0 \quad (3.8)$$

and so the kinetic energy of one particle is

$$\frac{1}{2}\hat{\boldsymbol{\pi}}^2 = -\frac{1}{2}(\mathbf{p} + \mathbf{A})^2 = -\frac{1}{2}(p^2 + \mathbf{p} \cdot \mathbf{A} + \mathbf{A} \cdot \mathbf{p} + A^2) \quad (3.9)$$

A *gauge transformation* changes the magnetic vector potential, but not the magnetic field. The number of possible gauge transformations is infinite, and it is often convenient to impose certain restrictions. A *Coulomb gauge* satisfies

$$\nabla \cdot \mathbf{A} = 0 \quad (3.10)$$

and will be assumed henceforth. If we also exploit the fact that

$$(\mathbf{a} \times \mathbf{b}) \cdot \mathbf{c} = (\mathbf{b} \times \mathbf{c}) \cdot \mathbf{a} \quad (3.11)$$

and apply this to equation (3.6), we get

$$\hat{\pi}^2 = \hat{p}^2 + 2\mathbf{A} \cdot \hat{\mathbf{p}} + \hat{A}^2 \quad (3.12)$$

$$= \hat{p}^2 + \mathbf{B} \times (\mathbf{r} - \mathbf{g}) \cdot \hat{\mathbf{p}} + \frac{1}{4} (\mathbf{B} \times (\mathbf{r} - \mathbf{g}))^2 \quad (3.13)$$

For a gauge origin \mathbf{g} in a magnetic field, the *physical angular momentum* $\hat{\mathbf{J}}_{\mathbf{g}}$ and the *canonical angular momentum* $\hat{\mathbf{L}}_{\mathbf{g}}$ shares a similar relationship as \mathbf{p} and $\boldsymbol{\pi}$:

$$\hat{\mathbf{J}}_{\mathbf{g}} = (\mathbf{r} - \mathbf{g}) \times \hat{\boldsymbol{\pi}} \quad (3.14)$$

$$\hat{\mathbf{L}}_{\mathbf{g}} = (\mathbf{r} - \mathbf{g}) \times \hat{\mathbf{p}} \quad (3.15)$$

This latter expression does not represent a physically meaningful quantity except when $\mathbf{B} = 0$. When this result is inserted into equation (3.13), we get

$$\hat{\pi}^2 = \hat{p}^2 + \mathbf{B} \cdot \mathbf{L}_{\mathbf{g}} + A^2 \quad (3.16)$$

where the term $\mathbf{B} \cdot \mathbf{L}_{\mathbf{g}}$ is zero if the momentum is entirely perpendicular to the magnetic field.

Finally, we can adjust the electronic Hamiltonian,

$$\hat{\mathcal{H}} = \frac{1}{2} \sum_i \boldsymbol{\pi}_i^2 + \sum_{i < j} \frac{1}{r_{ij}} + \hat{\mathcal{V}} \quad (3.17)$$

and see that the overall changes are minor. Similar arguments can be used to show that also the Hamiltonian is gauge origin independent [9].

3.2 Chemistry in strong magnetic fields

It has been discovered that in strong magnetic fields, certain phenomena that are otherwise regarded as impossible, can occur. One effect is that all matter is compressed. The kinetic energy of the system increases the overall energy in many cases, but can also induce bonding effects. One example to this is the so-called “atom-spaghetti”, which are long chains of hydrogen atoms.

Magnetic fields in the vicinity of 1 a.u. may produce some of the most interesting and diverse chemical phenomena. This is easily seen if we return to the electronic Hamiltonian with the canonical momentum operator $\hat{\mathbf{p}}$ from equation (2.9). If we use the more general momentum operator $\hat{\boldsymbol{\pi}}$ as defined in equation (3.5), we get

$$\hat{\mathcal{H}} = \frac{1}{2} \sum_i \left(\hat{\mathbf{p}}_i + \hat{\mathbf{A}}_i \right)^2 + \sum_{i<j} \frac{1}{r_{ij}} - \sum_{i,I} \frac{Z_I}{r_{iI}} \quad (3.18)$$

where for the sake of convenience we have ignored any additional terms due to an external potential and so on. Notice that as long as $\hat{\mathbf{A}}$ is small, the system is dominated by Coulomb forces and the canonical momentum. If $\hat{\mathbf{A}}$ is slightly bigger, the linear terms may be relevant, but when $\hat{\mathbf{A}}$ is on the same order of magnitude as the other terms, at about 1 a.u., all terms are equally important. In this regime, a multitude of possibilities exists, and several unknown chemical systems might be encountered [10]. For example, the orbital Zeeman term ($\mathbf{L} \cdot \mathbf{B}$) will introduce a splitting of the p -orbitals on the same order of magnitude as the Coulomb forces. It follows that interesting chemistry of a different nature may happen when magnetic interactions becomes as important as their electrostatic counterparts. Small molecules have received most attention, but with MP2 theory installed in the LONDON code, larger molecules can be probed as well.

It was recently discovered [11] that entities that are known to be anti-bonding in the absence of a magnetic field may be strongly bonding if the magnetic field is powerful enough. This phenomenon is known as *paramagnetic bonding* and occurs because the magnetic field compresses the orbitals. This is an entirely different sort of chemical bond, and unlike anything that can be replicated yet in lab.

Another curious effect is *paramagnetic stabilization*. Paramagnetic molecules are positively magnetized in a magnetic field, if the field is strong enough, the molecule will change from paramagnetic to diamagnetic. In this point, where $\frac{\partial E}{\partial B} = 0$, the molecule has a minimum energy. Therefore, it has been stabilized by the magnetic field.

3.2.1 Strong and weak fields

What constitutes strong and weak magnetic fields is largely a question of perspective. In daily life, we would certainly consider anything over 1T as strong – in that regime, diamagnetic repulsion can be felt by human hands and the combination of MRI-scanners and heavy metal objects have even caused deaths [12]. However, continuous ¹ magnetic field is dwarfed by what can be found on white dwarfs and neutron stars.

¹Pulsed magnetic fields up to several kilotesla have been achieved [13].

On such stellar objects, fields from a few hundred tesla and up to several megatesla are known to exist [14, pp. 896-906], [15].

3.3 Magnetic properties

A molecule may have a permanent magnetic dipole moment m_0 . This is the magnetic analogue of a permanent electric dipole moment. Likewise, a molecule has a polarizability which determines how strongly it is polarized in an electric field. The magnetic equivalent to this phenomenon is the magnetizability. However, where electric properties can be grasped intuitively, magnetic properties are often more abstract and describe physical phenomena that are difficult to understand. Some key concepts need to be established first. The *magnetic permeability* μ is analogous to electric permittivity. The vacuum permeability μ_0 is defined as $4\pi \cdot 10^{-7} \text{NA}^{-2}$ and the *magnetizability*² χ is

$$\chi \equiv 1 - \frac{\mu}{\mu_0} \tag{3.19}$$

$$\tag{3.20}$$

The magnetization \mathbf{M} is defined so that

$$\mathbf{M} = \chi \mathbf{B} \tag{3.21}$$

where \mathbf{B} is the strength of the external magnetic field. Magnetizability is an important concept: if it is positive, then a molecule is positively magnetized by external fields, and the molecule is *paramagnetic*. If negative, then the molecule is repelled by a magnetic field and the molecule is *diamagnetic*. Both these effects are usually very weak, and only in a very strong field is the repulsion or attraction observable with the naked eye. However, once the field becomes strong enough, diamagnetic repulsion can cause spectacular effects – one example is the famous “frog experiment”, where researchers made a live frog levitate in a field of about 16T [16].

3.3.1 Magnetizabilities

The energy of a system as a function of magnetic field can be written as a Taylor expansion in terms of the \mathbf{B} , where the indices referring to various combinations of

²This entity is also often referred to as magnetic susceptibility.

Cartesian coordinates:

$$E(\mathbf{B}) = E_0 + \frac{1}{2} \sum_{\alpha} J_{\alpha} B_{\alpha} - \frac{1}{2!} \sum_{\alpha\beta} \chi_{\alpha\beta} B_{\alpha} B_{\beta} + \frac{1}{3!} \sum_{\alpha\beta\gamma\delta} X_{\alpha\beta\gamma\delta} B_{\alpha} B_{\beta} B_{\gamma} + \dots \quad (3.22)$$

The angular momentum \mathbf{J} is the first derivative of energy with respect to magnetic field, the magnetizability χ is the second derivative, followed by the higher order hypermagnetizabilities X . All calculations in this thesis were performed with closed shell systems. In such cases, $E(\mathbf{B}) = E(-\mathbf{B})$, and all odd terms in the Taylor expansion are zero for reasons of symmetry. That leaves us with $\chi_{\alpha\beta}$ and $X_{\alpha\beta\gamma\delta}$

$$\chi_{\alpha\beta} = - \left. \frac{\partial^2 E(\mathbf{B})}{\partial B_{\alpha} \partial B_{\beta}} \right|_{\mathbf{B}=0} \quad (3.23)$$

$$X_{\alpha\beta\gamma\delta} = - \left. \frac{\partial^4 E(\mathbf{B})}{\partial B_{\alpha} \partial B_{\beta} \partial B_{\gamma} \partial B_{\delta}} \right|_{\mathbf{B}=0} \quad (3.24)$$

In this thesis, only the diagonal elements of the magnetizability and hypermagnetizability tensors are computed. Magnetizability is a rather abstract concept. Regarding it as the double derivative of energy with regards to the magnetic field has one unfortunate implication: in order to get the entire magnetizability tensor, we need *all* possible grid combinations of the magnetic field. If we are satisfied with 10 data points for each member of the tensor, we need 1000 calculations to be performed, whereas 30 are enough to get the diagonal elements. However, one can also regard the magnetizability as the first derivative of the momentum \mathbf{J} as introduced in equation (3.14). This approach has the propitious consequence that the off-diagonal tensor elements can be computed with a minimum of effort. Unfortunately, this approach relies on the Hellmann-Feynman theorem, which is not applicable in our case for two reasons. One is that the Hellmann-Feynman theorem is only valid for variational methods, which the MP2 method is not. However, as long as the system can be described reasonably with MP2 theory, then an estimate of χ which relies on the Hellmann-Feynman theorem will be *approximately* correct. The other reason is more insidious: we rely on London orbitals, and since these include the magnetic gauge, it can be shown that Hellmann-Feynman does not apply.

Computing magnetic properties

One way to determine the magnetic properties is to use response theory. High order response theory is prohibitively complicated to program and at the MP2 level, nobody has ever investigated magnetic response. Finite field is a much easier approach

to static properties, but for the calculations to be reliable, gauge origin invariant orbitals are a must. The body of this thesis revolved around implementing MP2 in the LONDON code, and so calculating magnetizabilities and hypermagnetizabilities at the MP2 level was deemed appropriate. Magnetizabilities and hypermagnetizabilities involve only a single perturbation, and are as such among the simplest response properties to calculate. Comparison of these values at HF and MP2 levels may provide insight into the importance of correlation effects in weak fields.

From a practical perspective, it simply entails a systematic variation of the magnetic field over a fixed geometry. The energy, as a function of magnetic field can then be fitted with a polynomial, and the coefficients of this polynomial multiplied with the Taylor factors are then representing magnetic properties order by order. The Taylor factor is $-\frac{1^{n+1}}{n!}$ for each order n [17].

3.4 Some pitfalls when dealing with magnetic fields

Since the Hamiltonian as such does not change, it means that all the methods we use are just as valid with a magnetic field as without. However, many of the frequently used short-cuts and assumptions cease to be valid. For example, a hermitian matrix with only real numbers is symmetric. Symmetric matrices have some very powerful properties that are highly advantageous from a numerical perspective. Some matrices, like the Hamiltonian matrix, are *always* real if the basis functions are real. Bringing such assumptions into the realm of complex values is bound to cause problems. For example, it is always true that

$$(pq|rs) = (rs|pq) \tag{3.25}$$

but if we know that the integral is real, we get the additional symmetries:

$$\begin{aligned} (pq|rs) &= (pq|sr) = (qp|rs) = (qp|sr) \\ &= (rs|qp) = (sr|pq) = (sr|qp) \end{aligned}$$

Exploiting this can speed up a calculation, and therefore it is “always” done, and many descriptions of various algorithms tacitly assume the real case. Such assumptions frequently break down when using complex orbitals. When developing new methods it is very important to keep track of the assumptions and approximations underlying the methods upon which the development is based.

Chapter 4

London orbitals and gauge invariance

Atomic and molecular orbitals are a somewhat artificial way of describing the electronic structure of atoms, but they are very practical and mostly correct.

4.1 Introduction to orbital theory

The exact wave-function is unknown, so we use linear combination of spinors that approximately it instead. There are two things to consider here. One is that the more the orbitals resemble the molecular system in question, the fewer orbitals are needed to produce a good description. This is important since most methods scale non-linearly with the number of basis functions. The other is that the orbitals in question should be of a kind that is easy to deal with mathematically. Typically, a certain kind of mathematical operation will be performed a great number of times, and if such operations can be performed analytically, CPU-time is greatly reduced.

The “proper” atomic orbital is a *contraction* of *primitive* functions.

$$u_k = \sum_{n=1}^m d_{nk} f_n \quad (4.1)$$

$$f_n = R(\mathbf{r}) S(\boldsymbol{\alpha}, \mathbf{r}) \quad (4.2)$$

Equation (4.1) describes an atomic orbital for an atom labeled k . This contracted orbital is a linear combination of basis functions whose form is described in equation (4.2). Here, $R(\mathbf{r})$ is a function describing the coordinates of the orbital. This is usually done by means of spherical harmonics as these functions have some very

powerful mathematical properties and can significantly speed up a calculation. However, LONDON only uses Cartesian basis functions. The function $S(\boldsymbol{\alpha}, \mathbf{r})$ describes the *shape* of the basis function. Three possible shapes are

$$\chi_{\text{STO}}(\mathbf{r}; \mathbf{R}, \zeta) = R(\mathbf{r}) \exp[-\zeta(\mathbf{r} - \mathbf{R})] \quad (4.3)$$

$$\chi_{\text{GTO}}(\mathbf{r}; \mathbf{R}, \zeta) = R(\mathbf{r}) \exp[-\zeta(\mathbf{r} - \mathbf{R})^2] \quad (4.4)$$

$$\omega_{\text{LGTO}}(\mathbf{r}, \mathbf{A}; \mathbf{R}, \zeta) = R(\mathbf{r}) \exp[-\zeta(\mathbf{r} - \mathbf{R})^2] \exp[-i\mathbf{A}(\mathbf{R}) \cdot \mathbf{r}] \quad (4.5)$$

where equations (4.3), (4.4) and (4.5) describe Slater, Gaussian and London-type orbitals respectively and ζ describes the shape of the orbital; the higher the value, the higher and steeper the shape. Slater-type orbitals (STO) have a shape which is close to the asymptotic decay of hydrogen-like wave-functions, but are tricky to deal with. For example, analytical integrals are unavailable, and a large number of costly numerical integrations must be performed instead. They see limited usage¹ and will receive no further attention in this thesis. Gaussian-type orbitals (GTO) are by far the most prevalent. They do not resemble the actual system very well, particularly close to the center and very far from the center. It is, therefore, often necessary to add extra functions for these regions. Figure 4.1 shows the shapes of an STO and a GTO.

The LONDON program relies on London orbitals, and may handle very large magnetic fields *intrinsically*. The London factor may be added to both GTOs (LGTO) and STOs (LSTO), but LONDON uses only the former. The mathematical expression for LGTOs is seen in equation (4.5). The London factor describes a vector potential at the center of the basis function. Note that in the absence of a magnetic field, the London factor is exactly one [18].

It should be noted that orbitals need not be described by any of the mentioned classes of functions. One can in principle use any set of functions, but it is advantageous if the members of that set resemble the actual system to as large a degree as possible – if the quality of a description quickly converges towards the system to be described, then a good approximation can be made from a linear combination of relatively few basis functions. When dealing with bulk systems, it is often advantageous to use plane waves [4].

4.2 Magnetic gauge and its implications

The magnetic vector potential was defined in equation (3.6). There are infinitely many different \mathbf{A} that may give the same magnetic field \mathbf{B} . However, not all mathe-

¹ADF is a notable exception.

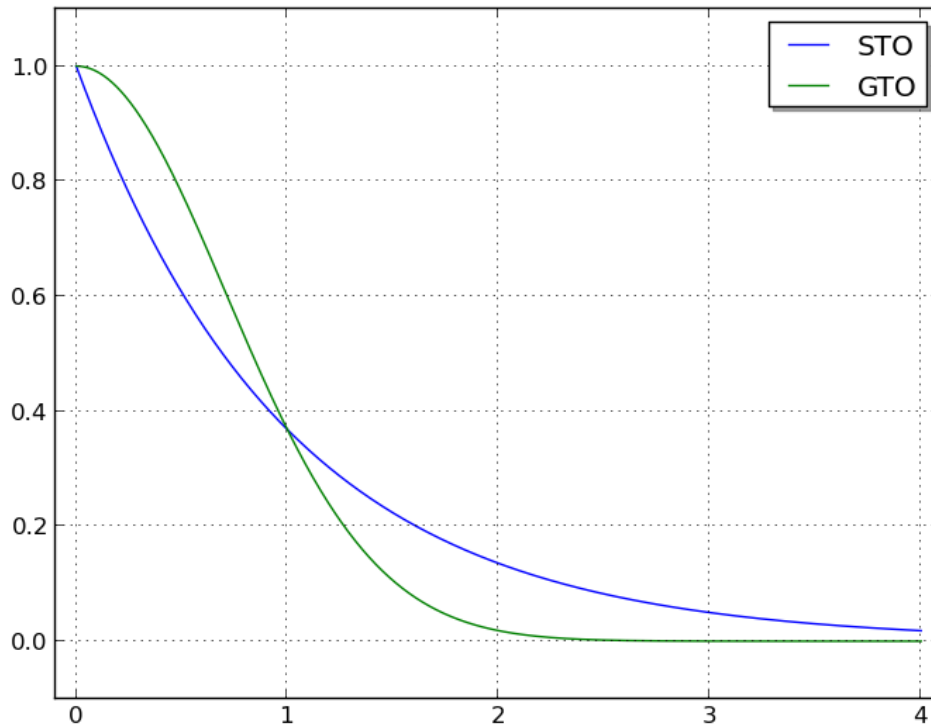


Figure 4.1: An STO and a GTO, both with all quantum numbers set to zero. The GTO does not diverge at $x = 0$ as it should and falls off too quickly. This image is simply an illustration of the general shape of the polynomials, hence the lack of labeling.

mational degrees of freedom of \mathbf{A} and \mathbf{V} correspond to a change in physically observable properties. Using an arbitrary $f(\mathbf{r})$:

$$\mathbf{A}' = \mathbf{A} + \nabla f(\mathbf{r}) \quad (4.6)$$

$$\phi' = e^{-if(\mathbf{r})}\phi \quad (4.7)$$

$$\boldsymbol{\pi}' = -i\nabla + \mathbf{A}' = \boldsymbol{\pi} + \nabla f(\mathbf{r}) \quad (4.8)$$

such a gauge transformation does not affect physical degrees of freedom. Example:

$$\hat{\boldsymbol{\pi}}'\phi' = (-i\nabla + \mathbf{A} + \nabla f)e^{-if(\mathbf{r})}\phi \quad (4.9)$$

$$= e^{-if(\mathbf{r})}(-i\nabla - \nabla f + \mathbf{A} + \nabla f) \quad (4.10)$$

$$= e^{-if(\mathbf{r})}(-i\nabla + \mathbf{A})\phi \quad (4.11)$$

$$= e^{-if(\mathbf{r})}\phi\hat{\boldsymbol{\pi}}\phi \quad (4.12)$$

$$\langle\phi'|\hat{\boldsymbol{\pi}}'|\phi'\rangle = \int\phi^*e^{if(\mathbf{r})}e^{-if(\mathbf{r})}\hat{\boldsymbol{\pi}}\phi\,d\mathbf{r} \quad (4.13)$$

$$= \int\phi^*\hat{\boldsymbol{\pi}}\phi\,d\mathbf{r} = \langle\phi|\hat{\boldsymbol{\pi}}|\phi\rangle \quad (4.14)$$

A similar approach can be used to show that $\hat{\mathcal{H}}$ and other relevant operators are gauge invariant as well. Hence, we are free to choose whichever gauge is most convenient, much like the origin of a Cartesian coordinate system is arbitrary. However, a gauge transformation will affect the phase of the wave-function and the Hamiltonian, but not the expectation value. Therefore;

$$\langle E\rangle = \langle\Psi|\hat{\mathcal{H}}|\Psi\rangle = \langle\Psi'|\hat{\mathcal{H}}'|\Psi'\rangle \quad (4.15)$$

While this does not correspond to an actual physical effect, it will affect a numerical approximation: both the orbitals and the Hamiltonian must be affected similarly by the gauge transformation. The Hamiltonian is trivial to adjust, but the orbitals must be represented in a basis. Hence, in the limit of an infinite basis, gauge invariance is exact. In practice, they are not. LGTOs include the gauge origin. For London- and Gaussian-type orbitals ($\omega_{\text{LGTO}}(\mathbf{r})$ and $\chi_{\text{GTO}}(\mathbf{r})$, respectively) in a uniform field \mathbf{B} ,

we get

$$\mathbf{A} = \frac{1}{2}\mathbf{B} \times (\mathbf{r} - \mathbf{g}) \quad (4.16)$$

$$\omega_{\text{LGTO}}(\mathbf{r}) = e^{-i\mathbf{A}(\mathbf{c})\cdot\mathbf{r}} \chi_{\text{GTO}}(\mathbf{r}) \quad (4.17)$$

$$= e^{-i\frac{1}{2}\mathbf{B}\times(\mathbf{c}-\mathbf{r})\cdot\mathbf{r}} \chi_{\text{GTO}}(\mathbf{r}) \quad (4.18)$$

$$\boldsymbol{\pi}\omega_{\text{LGTO}}(\mathbf{r}) = (-i\nabla + \mathbf{A}) e^{-i\mathbf{A}(\mathbf{c})\cdot\mathbf{r}} \chi_{\text{GTO}}(\mathbf{r}) \quad (4.19)$$

$$= e^{-i\mathbf{A}(\mathbf{c})\cdot\mathbf{r}} \left(-i\nabla - \frac{1}{2}\mathbf{B} \times (\mathbf{c} - \mathbf{g}) + \frac{1}{2}\mathbf{B} \times (\mathbf{r} - \mathbf{g}) \right) \chi_{\text{GTO}}(\mathbf{r}) \quad (4.20)$$

$$= e^{-i\mathbf{A}(\mathbf{c})\cdot\mathbf{r}} \left(-i\nabla - \frac{1}{2}\underbrace{\mathbf{B} \times (\mathbf{r} - \mathbf{c})}_{\mathbf{g} \text{ is gone}} \right) \chi_{\text{GTO}}(\mathbf{r}) \quad (4.21)$$

Similar results can be shown for $\hat{\mathcal{H}}$ and other relevant operators.

Therefore, London-type orbitals always provide exactly the same results, regardless of the gauge origin. It should be noted that London type orbitals are not enough by themselves for fields of arbitrary size: at some point, ignoring the relativistic effects will produce large errors. Therefore, most calculations in this thesis were restricted to fields lower than 2a.u., and no calculations were conducted above 10 a.u. Also, if the magnetic field is inhomogeneous, an even more general approach is required.

Chapter 5

Quantum Chemical methods

As discussed in chapter 1, some approximations are necessary. One of these is already mentioned; the Born-Oppenheimer approximation which freezes out the added complexities of the nuclei. However, pure electron calculations can be complicated enough all by themselves. There are numerous methods for calculating molecular properties; new ones are constantly being made and old ones refined, modified and tweaked for various purposes. In this chapter a brief overview over some methods will be discussed, as well as an attempt to place MP2 sensibly amongst them.

5.1 Hartree-Fock Theory

Hartree-Fock (HF) is a quantum chemical method developed in the late 1920s, and is the oldest many-body method produced that still sees extensive usage today [19]. The wave-function approximation is based on a single SD, as described in equation (2.15). A key concept to HF theory is the Fock operator

$$\hat{\mathcal{F}} = \sum_k \epsilon_k |\psi_k\rangle\langle\psi_k| \quad (5.1)$$

whose eigenvectors are the MO-coefficients. The HF procedure is about the optimization of the orbitals in the SD. This method is variational, so this is usually done iteratively: one start out with orbitals constructed from the canonical MOs, and iterate until the calculation has converged. Mathematically, we fill the MO-coefficients into a matrix \mathbf{C} so that

$$\mathbf{FC} = \mathbf{SC}\epsilon \quad (5.2)$$

where \mathbf{S} is the overlap matrix and ϵ the orbital energies. This system of equations is known as the Roothan-Hall equations. Determining the HF energy is therefore reduced to a series of eigenvalue evaluations, which is desirable from a numerical perspective [20].

It must be mentioned that Hartee-Fock theory exists in several different variants. Restricted Hartee-Fock theory (RHF) assume that all orbitals are filled with two electrons whenever possible. Therefore, all orbitals are used twice, one for each spin type electron. Logically, this setup works best for closed shell species. In Unrestricted Hartee-Fock theory (UHF), different orbitals are used for α and β electrons. We then get two Fock matrices, and two sets of equations that must be solved independently:

$$\mathbf{F}^{\alpha}\mathbf{C}^{\alpha} = \mathbf{S}\mathbf{C}^{\alpha}\epsilon^{\alpha} \quad (5.3)$$

$$\mathbf{F}^{\beta}\mathbf{C}^{\beta} = \mathbf{S}\mathbf{C}^{\beta}\epsilon^{\beta} \quad (5.4)$$

However, since the underlying ansatz is still based on a single SD, UHF suffers from *spin contamination*, which means that excited states interfere with the ground state. Another approach is the Restricted Open Hartee-Fock (ROHF) method, which relies on RHF as far as possible, and uses UHF for the remaining unpaired electrons. The most powerful method is probably the General Hartee-Fock (GHF) method, where there are no restrictions on the orbitals. Both RHF and UHF are special cases of GHF[21].

The HF method is size extensive and variational. It is also quite fast; it formally scales as N^4 , which is better than most other methods, and it is not very flop-intensive to begin with. With integral screening and other optimizations, it can be made to scale linearly. The main disadvantage is that it does not include correlation energy, and is therefore a less than optimal choice of method if highly accurate results are needed. Many phenomena, like dispersion, cannot be treated at all without including correlation energy. The method is also vulnerable to convergence problems in the SCF-procedure, but a good initial guess will obviate this obstacle.

A HF calculation will often provide a good starting point for more refined methods.

Post-Hartree-Fock methods

Many methods are based on HF, improving it in some way or another. These methods known as *post-Hartree-Fock methods*. Some common post-Hartree-Fock methods are Møller-Plesset perturbation theory (MPPT), Configuration Interaction theory (CI), Coupled Cluster theory (CC) and various compound methods.

5.2 Perturbative methods

One way to deal with the correlation energy is to treat it as a *perturbation* to the uncorrelated system.

5.2.1 Perturbation theory

Conceptually, perturbation theory attempts to simplify a complicated system by the following approximation: first, a system that is easier to deal with and which, to a large degree as possible, *resembles* the actual problem is assumed to be the *unperturbed* system. Then, the difference between the real system and the unperturbed system is treated as a *perturbation*. In other words, we get

$$\hat{\mathcal{H}}\Psi = \left(\hat{\mathcal{H}}_0 + \lambda\hat{\mathcal{H}}_I\right)\Psi \quad (5.5)$$

where $\hat{\mathcal{H}}$ is the actual Hamiltonian, $\hat{\mathcal{H}}_0$ the Hamiltonian for the unperturbed system and λ describes the strength of the perturbation $\hat{\mathcal{H}}_I$. There are two important assumptions at work here. One is that the perturbation is relatively small, i.e. that $\hat{\mathcal{H}}_0$ accounts for most of the energy. The other assumption is that the solutions of $\hat{\mathcal{H}}_0$;

$$\hat{\mathcal{H}}_0\Phi_i = E_i\Phi_i \quad \forall i \in \mathbb{N} \quad (5.6)$$

form a complete set. Since λ is a variable and $\hat{\mathcal{H}}$ is hermitian, it follows that both $\hat{\mathcal{H}}_0$ and $\hat{\mathcal{H}}_I$ by necessity must be hermitian as well. This in turn implies that the set of solutions to $\hat{\mathcal{H}}_0$ can be chosen to be orthonormal. The true solution

$$\hat{\mathcal{H}}\Psi = E\Psi \quad (5.7)$$

can now be written as a Taylor expansion of λ ;

$$W = \sum_{i=0}^{\infty} \lambda^i W_i \quad (5.8)$$

$$\Psi = \sum_{i=0}^{\infty} \lambda^i \Psi_i \quad (5.9)$$

corresponding to the unperturbed wave-function and eigenvalue plus all the higher order corrections. Since the set of $\{\Phi_0, \Phi_1, \dots\}$ is complete and orthonormal and a member of Hilbert space, it follows that $\langle \Psi | \Phi_i \rangle = 1 \forall \Phi_i$. Also keep in mind that

this must hold true for all values of λ , allowing us later to separate the equations order by order. Reinserting equations (5.8) and (5.9) into equation (5.7) we get

$$\left(\hat{\mathcal{H}}_0 + \lambda\hat{\mathcal{H}}_I\right) \sum_{i=0}^{\infty} \lambda^i \Psi_i = \left(\sum_{j=0}^{\infty} \lambda^j W_j\right) \left(\sum_{i=0}^{\infty} \lambda^i \Psi_i\right) \quad (5.10)$$

Sorting this by the order of λ , the i th order correction becomes

$$\hat{\mathcal{H}}_0 \Psi_i + \hat{\mathcal{H}}_I \Psi_{i-1} = \sum_{j=0}^i W_j \Psi_j \quad (5.11)$$

Notice that the zeroth order perturbation is reduced to the Schrödinger equation for the unperturbed system. In the limit where all corrections up to infinite order are included, this is exactly true, but of course, that is hardly an improvement. However, this series of corrections can be truncated at any point. This has several appealing consequences. Chief amongst them is that the level of accuracy can be chosen rather arbitrarily, and if higher accuracy or lower cost is required, a different truncation may be used. Since our chosen normalization requires that

$$\langle \Psi_i | \Phi_0 \rangle = \begin{cases} 0 & \forall i \neq 0 \\ 1 & \text{if } i = 0 \end{cases} \quad (5.12)$$

then multiplying equation (5.11) from the left with $\langle \Phi_0 |$ allows us to pick out the expression for W_i directly:

$$W_i = \underbrace{\langle \Phi_0 | \hat{\mathcal{H}}_0 | \Psi_i \rangle}_0 + \langle \Phi_0 | \hat{\mathcal{H}}_I | \Psi_{i-1} \rangle \quad (5.13)$$

This can be exploited even further; Wigner's $(2n + 1)$ -rule states that for each order n to which the perturbed wave-function is computed, the expectation value of the perturbed Hamiltonian can be calculated to order $2n + 1$ [22]:

$$W_{2n+1} = \langle \Psi_n | \hat{\mathcal{H}}_I | \Psi_n \rangle - \sum_{k,l=0}^n W_{2n+1-k-l} \langle \Psi_k | \Psi_l \rangle \quad (5.14)$$

At this point, the problem is that both the λ 's, energies and wave-function corrections are undetermined. We therefore need a systematic setup for finding these. Our

fundamental assumption is that we have everything we need for finding the reference energy;

$$W_0 = \langle \Phi_0 | \hat{\mathcal{H}}_0 | \Psi_0 \rangle \quad (5.15)$$

which can then be used for finding first order contributions.

$$|\Psi_1\rangle = \sum_i c_i |\Phi_i\rangle \quad (5.16)$$

$$(\hat{\mathcal{H}}_0 - W_0) |\Psi_1\rangle = (\hat{\mathcal{H}}_1 - W_1) |\Phi_0\rangle \quad (5.17)$$

$$\text{We multiply both sides by } \langle \Phi_0 | : \quad (5.18)$$

$$\Rightarrow W_1 = \langle \Phi_0 | \hat{\mathcal{H}}_1 | \Phi_0 \rangle \quad (5.19)$$

The clue here is that even though we don't yet know the expansion coefficients c_i for Ψ_1 , we do not need them to find W_1 . And, with W_1 in place, they are now the only set of unknowns in the equation, and we can find them without too much hassle:

$$c_i = \frac{\langle \Phi_j | \hat{\mathcal{H}}_I | \Phi_0 \rangle}{E_0 - E_j} \quad \forall i > 0 \quad (5.20)$$

The first order corrections can then be used to find the second order corrections and so on. The expressions quickly become very complicated, so we only state W_2 as we shall use this one later:

$$W_2 = \sum_{i \neq 0} \frac{\langle \Phi_0 | \hat{\mathcal{H}}_I | \Phi_i \rangle \langle \Phi_i | \hat{\mathcal{H}}_I | \Phi_0 \rangle}{E_0 - E_j} \quad (5.21)$$

Of course, this expression breaks down in the case of degeneracies, but that can be amended by various means.

5.2.2 Møller-Plesset perturbation theory (MPPT)

The missing feature from HF theory is correlation energy. This value typically is significant, which violates the assumption that a perturbation should be small. However, with a good starting extent, such as what is provided from a HF calculation, this is rarely a problem. We define $\hat{\mathcal{H}}_0$ in terms of the Fock-operator from equation (5.1):

$$\hat{\mathcal{H}}_0 = \sum_i \hat{\mathcal{F}}_i \quad (5.22)$$

A Fock-operator sees an average field of electron-electron repulsions. Since we sum over all electrons, but the repulsions are between electron pairs, this value is doubled. At this point, we recall that the eigenvalues of the Fock-operator are the orbital energies. Therefore, if we insert the above equation into equation (5.15) we see that W_0 is simply the sum of orbital energies;

$$W_0 = \sum_i \epsilon_i \quad (5.23)$$

The first order correction is $W_1 = \langle \Phi_0 | \hat{\mathcal{H}}_I | \Phi_0 \rangle$. In short, the unperturbed MPPT solution is the orbital energies, and if we add the first order perturbation, we get the HF energy. Simply put, MPPT to first order is nothing but a reformulation of the HF method – a reformulation that relies on the HF method for finding the orbitals to begin with. Clearly, MPPT is only interesting for higher order perturbations. The implementations in this thesis deal exclusively with second order corrections, so we will limit our attention to that. We must now consider the singly excited SDs;

$$|\Phi_i^a\rangle = \hat{a}_a^\dagger \hat{a}_i |\Phi_0\rangle \quad (5.24)$$

$$\langle \Phi_0 | \hat{\mathcal{H}}_0 | \Phi_i^a \rangle = 0 \quad (5.25)$$

$$\langle \Phi_0 | \hat{\mathcal{H}}_I | \Phi_i^a \rangle = 0 \quad (5.26)$$

and the doubly excited SDs:

$$|\Phi_{ij}^{ab}\rangle = \hat{a}_a^\dagger \hat{a}_b^\dagger \hat{a}_i \hat{a}_j |\Phi_0\rangle \quad (5.27)$$

The summation can be reduced significantly by restricting the summation to the possible excitations. In LONDON, classical MP2 was implemented only for a RHF starting point. In this case, only the indices of the two-electron integrals matter.

$$W_2 = \sum_{i < j}^F \sum_{a > b = F}^N \frac{\langle \Phi_0 | \hat{\mathcal{H}}_I | \Phi_{ij}^{ab} \rangle \langle \Phi_{ij}^{ab} | \hat{\mathcal{H}}_I | \Phi_0 \rangle}{E_0 - E_{ij}^{ab}} \quad (5.28)$$

$$(ia | jb) = \int i(1)j(2) \frac{1}{r_{12}} a(1)b(2) dr_1 dr_2 \quad (5.29)$$

$$\Rightarrow W_2 = \sum_{i,j,a,b} \frac{2|(ai | bj)|^2 - (ai | bj)(ib | aj)}{\epsilon_a + \epsilon_b - \epsilon_i - \epsilon_j} \quad (5.30)$$

$$E_{\text{MP2}} = E_{\text{HF}} - W_2 \quad (5.31)$$

[23, 7]

Advantages and disadvantages

All quantum chemical methods have their strengths and weaknesses. Some advantages to MPPT methods are:

- MPPT-methods are size extensive.
- Speed. MP2 formally scales as N^5 , which is very good: MP2 is canonically the fastest *ab initio* method that can calculate dynamic correlation.
- Ease of implementation. The method itself is easy to implement, and can be a useful addition to programs that already have more sophisticated methods implemented.
- Several highly accurate composite methods use various contributions from MPPT-methods. Thus, a proper implementation can be reused.

There are some drawbacks to MPPT-methods as well, including

- MPPT-methods are not variational. This, however, is more of a missing feature than actual flaw, and it holds true for a lot of methods, the CC-family included.
- Methods founded on MPPT cannot be systematically improved simply by adding higher order perturbations – in the absence of an infinite basis, results will at some point diverge. However, results *can* be improved systematically consequently get better results since there is a close link between MPPT methods and couple cluster methods. This will be explained briefly in section 5.3.2.

5.3 Two other methods worth mentioning

Quantum chemical methods often share some key principles, or are in some way logically related. Understanding related methods provides a valuable insight into the common mathematical formulation of the field. Of particular interest is Coupled Cluster theory since it is a logical extension to Møller-Plesset perturbation theory. Configuration Interaction theory is also important to see in relation with the others.

5.3.1 Configuration Interaction theory

In Configuration Interaction theory (CI), the wave function is written as a linear combination of determinants where the HF wave function is the first term:

$$\Psi_{\text{CI}} = C_0 \Psi_{\text{HF}} + \sum_{ai} C_i^a \Psi_i^a + \sum_{abij} C_{ij}^{ab} \Psi_{ij}^{ab} + \dots \quad (5.32)$$

The wave function ansatz Ψ_{CI} is which is sorted by number of excitations. The problem to be solved is reduced to determining the expansion coefficients C . These coefficient are variationally determined. The elements of the CI-matrix \mathbf{H} is simply

$$H_{mn} = \langle \Psi_m | \hat{\mathcal{H}} | \Psi_n \rangle \quad (5.33)$$

which leaves us with set of secular equations;

$$\mathbf{HC} = EC \quad (5.34)$$

Solving these equations entails diagonalizing the CI matrix, whose lowest eigenvalue is the ground state energy of the system.

It is possible to truncate the series of excitations, or one can include all of them. This gives rise to two different methods: full CI (FCI) and truncated CI. The latter is given its name depending on where it is truncated. For example CISDT includes singles, doubles and triples. Mathematically, the difference between truncated CI methods and the FCI method is small, but practical implications are enormous: truncated CI methods are not size-extensive. It also depends on reference orbitals (which in practice will always be HF orbitals). FCI has neither of these restrictions. Truncated CI methods see little usage, but FCI is extremely useful. In this thesis, FCI¹ was used for comparing and validating results produced with MP2. FCI is possibly the most accurate method available, and it is easy to implement. The only drawback is that it is extremely slow for all but the smallest systems: it does not scale in polynomial time, not even exponentially – the scaling is *factorial* with the system size.

5.3.2 Coupled cluster theory

In coupled cluster (CC) theory, the cluster operator $\hat{\mathcal{T}}$ is very similar to the correlation operator found in perturbation theory. Here, the unknown variables that need to be identified are the cluster amplitudes \hat{t}_H^P .

$$\begin{aligned} |\Psi_{CC}\rangle &= e^{\hat{\mathcal{T}}} |\Phi_0\rangle \\ &\approx \sum_{n=1}^N \frac{1}{n!} \hat{\mathcal{T}}^n |\Phi_0\rangle \\ \hat{\mathcal{T}}^n &= \left(\frac{1}{n!}\right)^2 \sum_{ijk\dots n, abc\dots n} t_{ijk\dots n}^{abc\dots n} \hat{a}_a^\dagger \hat{a}_b^\dagger \hat{a}_c^\dagger \dots \hat{a}_n^\dagger \hat{a}_i \hat{a}_j \hat{a}_k \dots \hat{a}_n \end{aligned}$$

¹FCI is implemented as a sub-routine in the CAS-solver in LONDON.

If a CC calculation were to be performed for all possible excitations, it would simply be a complicated way of doing FCI. However, when truncated, the difference becomes apparent: as previously mentioned, truncated CI methods are not size-extensive, but they are variational. For truncated CC methods, the situation is exactly the opposite; the methods are size-extensive, but not variational[24].

CC theory revolves around determining amplitudes. This can be seen as a minimization problem, and is usually done iteratively. This is where the link to MPPT becomes evident: MP2 describes the single and double excitations perturbatively. Coupled cluster at the corresponding level (CCSD) treats these values in an iterative fashion – the MP2 contribution is simply the results from the first iteration in a CCSD-calculation. The beauty of coupled cluster methods lies in the exponential Taylor ansatz: adding higher order contributions does not cause divergence like higher order perturbations in MPPT. There is also a natural system here; the triples can be treated as a perturbation to the doubles, which results in CCSD(T). Then, if even better results are required, we can solve the amplitudes for the triples iteratively as well, a method known as CCSDT. This can then be improved step by step until all possible excitations are included. However, this setup scales as N^{4+2k+p} where k is the number of excitations beyond singles and p is either 1 or 0 depending on whether perturbative expansions are added or not. A higher order coupled cluster calculation quickly becomes prohibitively expensive for all but the smallest systems, but it can provide extremely accurate results in cases where FCI is impossible.

Part III

Implementation and results

Chapter 6

Implementation

I have implemented MP2 theory in the LONDON code in two different variants. One is a classical MP2 method as described in section 5.2.2. This was implemented in the CAS-CI/CAS-SCF-code, and also as a free-standing class.

The other implementation is of Laplace-MP2 theory. This was the most work intensive and difficult programming endeavor.

6.1 Implementation of classical MP2

Since LONDON has several modules for performing two-electron integrals and doing SCF-optimization, almost everything needed to implement an MP2 method was already available. It was implemented in three different places, but in a very similar way. First, when CAS-SCF and CAS-CI calculations are run, the MP2-energy is printed rather early in the routine. This is done on the grounds that MP2 is much faster than either of these methods and because CAS-type methods does not compute dynamic correlation unless all excitations are included (which in effect is FCI). The MP2 method was also implemented as a free-standing module.

The actual MP2 contribution to the energy as implemented in LONDON is seen in Code 6.1. This method was implemented and compared with the MP2 method of DALTON, CCSD in LONDON and FCI. When the veracity of the method was confirmed, Laplace-MP2 was implemented. That way, all results produced could easily be checked against a known, working method in the same program, which greatly facilitated debugging and testing.

```
1 int ix, jx, ax, bx;
2 for (ix = 0; ix < num_occ_orb; ix++) {
3   for (jx = 0; jx < num_occ_orb; jx++) {
4     for (ax = num_occ_orb; ax < num_orb; ax++) {
5       for (bx = num_occ_orb; bx < num_orb; bx++) {
6         MP2_tweights = cint->get_twoint(ax, ix, bx, jx);
7         MP2_tweights *= qc<cnum_t>::conjg(MP2_tweights);
8         MP2_tweights_ex = cint->get_twoint(ax, ix, bx, jx)
9           *cint->get_twoint(ix, bx, jx, ax);
10        OrbEloc =
11          - OrbEnergy->e_const(ix, 0)
12          - OrbEnergy->e_const(jx, 0)
13          + OrbEnergy->e_const(ax, 0)
14          + OrbEnergy->e_const(bx, 0);
15        MP2.E += ((cnum_t(2.0)*MP2_tweights
16          - MP2_tweights_ex)/OrbEloc);
17      }
18    }
19  }
20 }
```

Code 6.1: Simple evaluation of the MP2-contribution. In this case, all two-electron integrals were already available.

6.2 Implementation of Laplace-MP2

The implementation of Laplace-MP2 was much more time consuming since the algorithm is more complicated.

6.2.1 The Laplace transform ansatz

The expression for the MP2 contribution was outlined in equation (5.30). However, computing the two-electron integrals

$$(ia | jb) = \left\langle i(1)j(2) \left| \frac{1}{r_{12}} \right| a(1)b(2) \right\rangle \quad (6.1)$$

is associated with a costly transformation from molecular orbitals (MO) to atomic orbitals (AO),

$$(ia | jb) = \sum_{\nu\mu\chi\lambda} (\nu\mu | \chi\lambda) C_{\nu i}^* C_{\mu a} C_{\chi j}^* C_{\lambda b} \quad (6.2)$$

which is the step that scales as N^5 , where N is the number of basis functions. The Laplace transform ansatz circumvents this step and everything is done in the AO basis. Writing this denominator as

$$x = \epsilon_a + \epsilon_b - \epsilon_i - \epsilon_j \quad (6.3)$$

where i, j are occupied orbitals of the ground state and a, b virtual, the values can be brought over to the AO basis by means of a Laplace transformation. Thus, we get

$$\frac{1}{x} = \int_0^\infty e^{-xt} dt \approx \sum_{\alpha=0}^{\tau} w_\alpha e^{-xt_\alpha} \quad (6.4)$$

where w are the integration weights and the values of t are some reasonable exponents. This ansatz was first proposed by Almlöf in 1991 [25].

6.2.2 Implementing the Laplace-MP2 algorithm

The algorithm, as described by Häser [26],¹ is a sequential recipe where the critical components can be implemented independently. The algorithm will be explained

¹We chose the in-core, multiple pass variant.

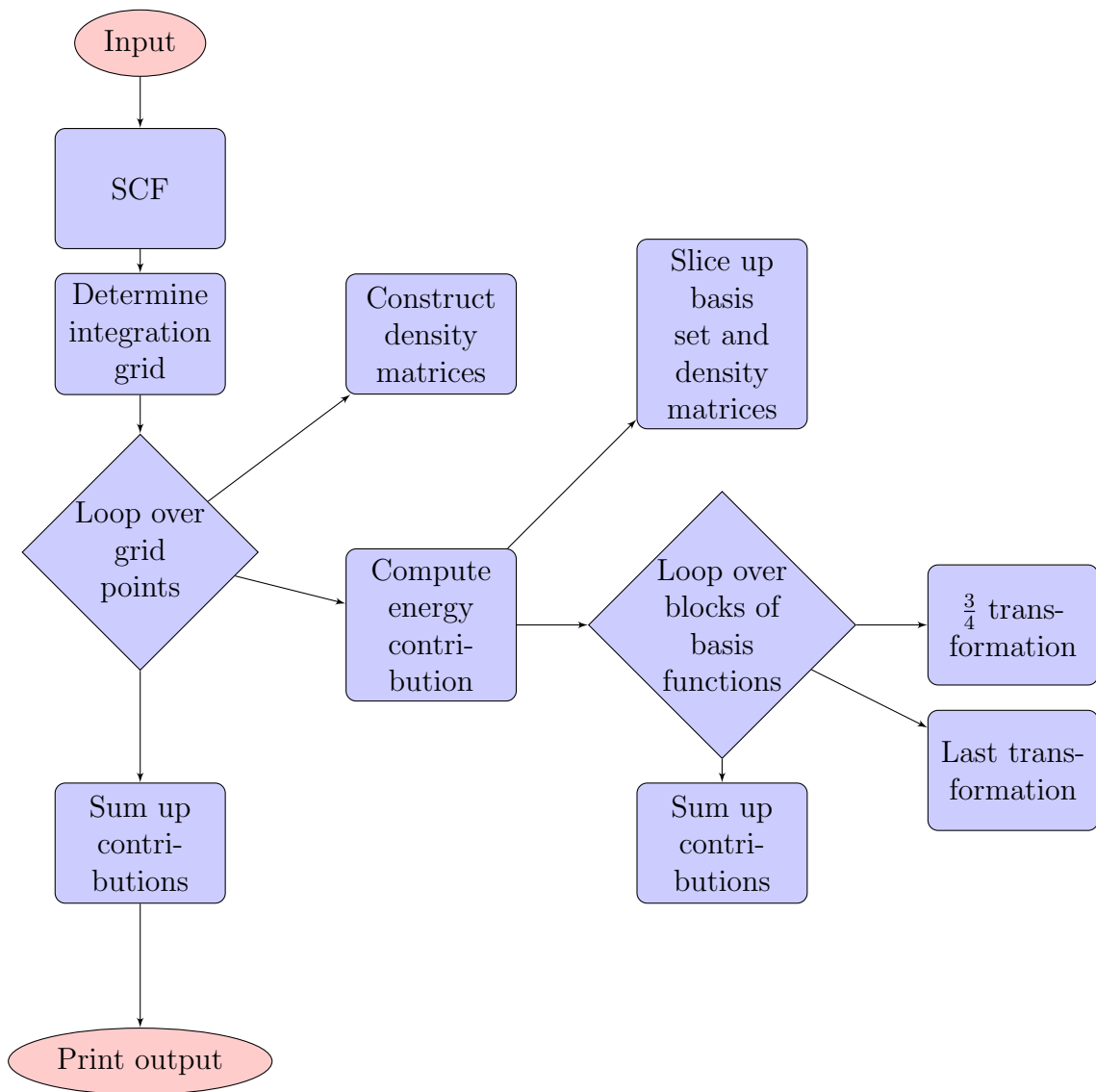


Figure 6.1: The L-MP2 algorithm as implemented. Each box defines a natural part or function of the code.

step by step as it is implemented in the LONDON code. This is largely done in accordance with Häser's description, but some modifications are involved. A simple sketch of the algorithm is seen in figure 6.1. It must be stressed that this is a pilot implementation, and it is not fully optimized.

6.2.3 Setting up the calculation and fitting

First, a regular HF calculation is run to get the HF-orbitals. With these in store, the integral weights are computed. This is determined by a least squares condition;

$$\int_{x_{\max}}^{x_{\min}} f(x) \left[\frac{1}{x} - \sum_{\alpha=1}^{\tau} w_{\alpha} e^{-xt_{\alpha}} \right]^2 dx = \min! \quad (6.5)$$

This can be solved as a simple matrix problem

$$\mathbf{A}\mathbf{W} = \mathbf{C} \quad (6.6)$$

where \mathbf{W} represents the needed weights. Due to numerical instability, we took an extra step of matrix decomposition. Since \mathbf{A} by necessity must be hermitian, it is also square and positive-definite. Assuming all capital letters are matrices, and that \mathbf{a} represents the eigenvalues of \mathbf{A} , the following substitution is possible:

$$\mathbf{A} = \mathbf{U}\mathbf{a}\mathbf{U}^{\dagger} \quad (6.7)$$

$$\mathbf{U}\mathbf{a}\mathbf{U}^{\dagger}\mathbf{W} = \mathbf{C} \quad (6.8)$$

$$\Rightarrow \mathbf{W} = \mathbf{U}\mathbf{a}^{-1}\mathbf{U}^{\dagger}\mathbf{C} \quad (6.9)$$

For such operations, we use routines from the Lapack library. These routines are highly optimized and extremely fast. Since \mathbf{a} is diagonal, it is easy to invert. However, if certain elements of \mathbf{a} are very small, they will not contribute much to the overall result, but it may cause numerical instability. Therefore, we filter those offending values away and set their contribution to zero.

Defining the grid over which the integration should take place is non-trivial. Initially, it was assumed that a bad fitting procedure would merely provide slower convergence or results of inferior quality at increased cost, but otherwise not be that critical. It was certainly not expected to provide results that were uniformly wrong and where the number of integration points held little or no promise of convergence. Evidently, we must also have good exponents t to insert in equation (6.4). A reasonable assumption for a two point fitting is one where the approximation replicates

both end points and the first derivative in these points. Since

$$\frac{\left(\frac{de^{-xt}}{dt}\right)}{e^{-xt}} = \frac{x^{-2}}{x^{-1}} \quad (6.10)$$

$$t = \frac{1}{x} \quad (6.11)$$

we can simply insert the endpoints as

$$t_A = \frac{1}{x_{\max}} \quad (6.12)$$

$$t_B = \frac{1}{x_{\min}} \quad (6.13)$$

where max and min refers to highest and lowest value of x . It turned out that a linear grid between these two points was not sufficient. Therefore, the following solution was implemented: the grid between t_A and t_B was stretched out by a factor $\lfloor \frac{N}{3} \rfloor$. If seven grid points ($N = 7$) were requested, then there would be one point at these two locations, three in between, and two extra *beyond* t_2 :

$$a = t_A \quad (6.14)$$

$$l = \lfloor \frac{N}{3} \rfloor \quad (6.15)$$

$$t_B = ab^{N-1-l} \quad (6.16)$$

$$t_{B+k} = ab^{N-1-l}b^k \forall k \leq l \quad (6.17)$$

so that the fitting got more points in the region where the curve is steepest. The spacing between the points is regular, but the extra points have a value based on a logarithmic approach.

Once the integration points are computed, the energy contribution for each point can be determined independently of the others. This is by far the most time consuming part of a calculation and there is no need for intercommunication – each contribution is summed up to a total estimate of the energy of the system. As such, this loop can be parallelized without any further ado. Of course, there is little need to go beyond 8-10 weight points, so even though the algorithm could be efficiently implemented in a distributed fashion at this point, there is little practical purpose in doing it. However, for local calculations on a multicore machine, this is excellent news. Parallelization is not implemented as of today.

The energy weighted density matrices

The $\overline{\mathbf{D}}$ and $\underline{\mathbf{D}}$ -matrices describe the occupied-occupied and virtual-virtual blocks of the exponential of Fock matrix. This setup allows for a frozen core, but that is not part of our implementation. These matrices are needed for the transformations, and must be computed first.

$$\overline{\mathbf{D}}_{\nu\mu}^{(\alpha)} = \sum_i C_{\nu i} e^{t_\alpha(\epsilon_i - \epsilon_F)} C_{\mu i}^* \quad (6.18)$$

$$\underline{\mathbf{D}}_{\nu\mu}^{(\alpha)} = \sum_a C_{\nu a} e^{t_\alpha(\epsilon_F - \epsilon_a)} C_{\mu a}^* \quad (6.19)$$

This is an example where things becomes different when dealing with orbitals that are inherently complex: with the London factor and a magnetic field, the MO coefficients \mathbf{C} are complex. In more regular implementations, they are real ² and so there was no complex conjugation of the equivalent of these equations in the original recipe. These matrices will be sparse if the electrons are well localized, a property that can be exploited in the name of celerity [27].

Computing the energy contributions

The next step is to calculate the energy contribution at the point t_α . First, the D-matrices are decontracted in order to fit a primitive basis set. This is not strictly necessary, but it makes it much easier to split the basis set later in the procedure. This is important if the system requires a lot of memory, and the splitting itself is not very time consuming.³ The splitting of the basis set simply entails looping over the number of *primitive centers*. In practice a primitive center corresponds to a shell with a specific principal quantum number n . If $n > 1$, then the azimuthal quantum number l assumes different values. It is sufficient to calculate the integrals for to the highest angular momentum as all the others are provided as intermediary steps in the calculation thereof. This only holds true if all the orbitals belonging to the n in question are kept together. If the basis is split on a center, then these redundant integral evaluations must be performed anyway. We add centers together until they form a block of predefined size, and loop over all pairs of blocks in order to get all

²They need not be real, but they can be chosen to be real. Real numbers are easier to deal with, so this is done whenever it is possible.

³A proper splitting can in theory allow calculations of arbitrary size to be performed, the only restriction being total available CPU time.

the contributions. The energy contribution of one integration point t_α is

$$e_\alpha = \sum_{\nu\mu\chi\lambda} (\bar{\nu}\underline{\mu} | \bar{\chi}\underline{\lambda}) [2(\nu\mu | \chi\lambda) - (\nu\lambda | \chi\mu)] \quad (6.20)$$

where (for each α)

$$|\bar{\nu}\rangle = \sum_{\mu} |\mu\rangle \bar{\mathbf{D}}_{\mu\nu} \quad (6.21)$$

and $|\nu\rangle$ is a basis function in the AO-basis. These relate to the MO basis so that

$$|p\rangle = \sum_{\nu} |\nu\rangle C_{\nu p} \quad (6.22)$$

as usual. At this point, the expression for the energy contribution is set, and the next logical step is to do the transformations so that $(\bar{\nu}\underline{\mu} | \bar{\chi}\underline{\lambda})$ can be computed. However, the total transformation process is split into two different modules. One performs the first three quarter of the total transformation, producing $(\bar{\nu}\underline{\mu} | \bar{\chi}\underline{\lambda}')$ while the second deals with the last step. This splitting is simply a convenient way of facilitating the future implementation of integral screening.

The two-electron integral tensor with the entire basis and the second of the two chosen blocks (M2) of basis functions is computed. We exploit equation (3.25) so that M2 can be put in the second place. This leads to numerical efficiency: the `TensorND` objects are row-major, while the `Matrix` objects are column-major. This corresponds to the typical setup in C-type languages and FORTRAN, respectively. In essence, it is a question of whether the left or right index should be the innermost index in a loop.⁴ Since implementing the necessary equation often entails both `Matrix` and `TensorND` objects, such tricks are necessary for reducing CPU-time. For contraction, we need both the entire transposed $\bar{\mathbf{D}}$ -matrix and the part of it which corresponds to the block M2 of the basis set.

Finally, it is time for the transformations. The original integral tensor is contracted with the decontracted $\underline{\mathbf{D}}$ matrix and the relevant slice of $\bar{\mathbf{D}}$. The result is transposed, contracted with the *entire* $\bar{\mathbf{D}}^T$, and transposed back again. The next step of the algorithm is a bit counter intuitive. An expression that superficially resembles equation (6.20) is calculated, but the last contraction is withheld

$$\bar{\mathbf{R}}_{\lambda,\lambda'}(M, M') = \sum_{\nu \in M} \sum_{\mu, \chi} (\bar{\nu}\underline{\mu} | \bar{\chi}\underline{\lambda}') [2(\nu\mu | \chi\lambda) - (\nu\lambda | \chi\mu)] \quad (6.23)$$

```

1  TensorND<4, cnum_t> h_rsPQ;
2  if (!h_rsPQ.contract_last_idx_pair(g_rspq, DMoverT, *D_underbar_prim)) {
3      qout << "lmp2::threequarter_transform: failed to contract h_rsPQ" << endl;
4      return false;
5  }
6  g_rspq.reset(); // don't need g_rspq anymore, free memory!
7  TensorND<4, cnum_t> h_sPQr_hreord;
8  if (!h_sPQr_hreord.transpose(h_rsPQ, 1)) {
9      qout << "lmp2::threequarter_transform: transpose h_sPQr_hreord failed"
10         << endl;
11     return false;
12 }
13 h_rsPQ.reset(); // don't need it anymore, free memory!
14 TensorND<4, cnum_t> g_sPQR_reord;
15 if (!g_sPQR_reord.contract_last_idx(h_sPQr_hreord, D_overbarT)) {
16     qout << "lmp2::threequarter_transform: failed to contract g_sPQR_reord"
17         << endl;
18     return false;
19 }-
20 h_sPQr_hreord.reset(); // don't need it anymore, free memory!
21 if (!g_PQRs.transpose(g_sPQR_reord, 1)) {
22     qout << "lmp2::threequarter_transform: failed to transpose h_sPQr_hreord"
23         << endl;
24     return false;
25 }
26 return true;

```

Code 6.2: These are the final steps of the $\frac{3}{4}$ -routine, and where the actual transformations of the integral tensor takes place.

```

1  for (int S = 0; S < N_prim; S++) {
2    for (int s = 0; s < m2_end-m2_start; s++) {
3      cnum_t tmp = cnum_t(0.0);
4      for (int P = 0; P < m1_end-m1_start; P++) {
5        for (int Q = 0; Q < N_prim; Q++) {
6          for (int R = 0; R < N_prim; R++) {
7            tmp+=(g_QPSR.e(Q,P,S,R)-0.5*g_QRSP.e(Q,R,S,P))*g_PQRs.e(P,Q,R,s);
8          }
9        }
10       }
11       R.e(S, s) = tmp;
12     }
13  }

```

Code 6.3: Adding up the contributions from the chosen pair of basis set blocks, preparing for the last contraction to be performed.

which is carried out in the function `make_R`. Code 6.3 shows the relevant excerpt.

$$E_{\text{MP2}} = \sum_{\alpha=1}^{\tau} w_{\alpha} e_{\alpha} \quad (6.24)$$

The next step is to perform the last transformation (code 6.4) and sum up the

```

1    for (int S = 0; S < N_prim; S++){
2      for (int s = 0; s < m2_end - m2_start; s++) {
3        e_M1_M2 += R.e(S, s) * D_underbar_prim.e(m2_start+s, S);
4      }
5    }
6    energy += real_t(2.0) * qc<cnum_t>::real_part(e_M1_M2);

```

Code 6.4: Last contraction. `S` runs over the total number of primitive basis functions while `s` runs over the block `M2`.

contributions from each pair of basis set blocks. The energy contribution from one weight point is now complete, and when all these contributions are added together, the evaluation of the MP2 energy is complete.

⁴This is due to memory allocation: array iterations are can be performed much faster if the memory addresses of the values are logically ordered.

6.2.4 Integral screening

There are many integral evaluations that need to be performed. If one can determine *a priori* that a certain costly calculation by necessity must be smaller than some acceptance criteria – for example some typical error inherent to the method employed – then it is not necessary to waste time computing the integral in question. The AO-basis is ideal for integral screening since the chosen orbitals corresponds to a specific atom, and thus a position in the molecule – quite unlike the MO-basis, where each orbital is a linear combination of all the AO-orbitals of the system. If an orbital has a localized position in space, we can safely exclude interactions with orbitals that are sufficiently far away. AO-MP2 with integral screening can be used to perform calculations on large bio-molecules with thousands of atoms with a 6-31G** basis set [28].

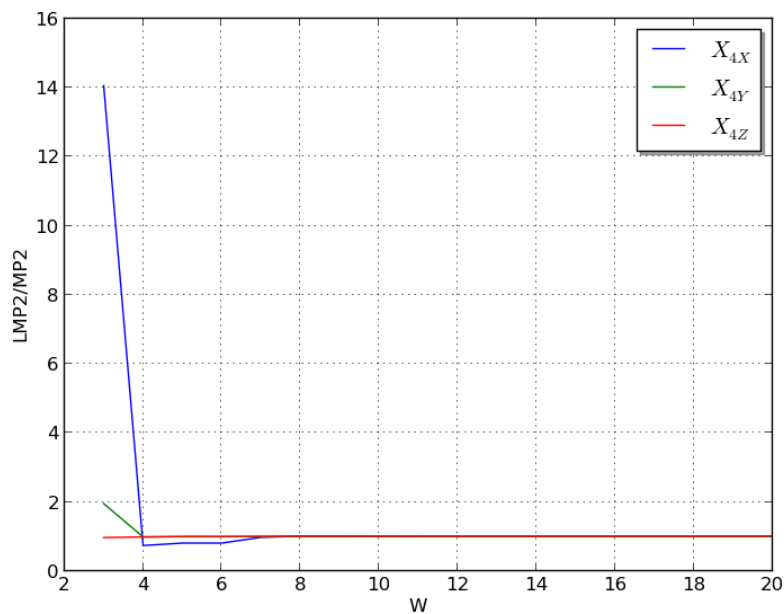
6.2.5 A small test case

In order to determine the quality of a Laplace-MP2 calculation based on the number of weights, then it makes most sense to compare the Laplace-MP2 energy with the MP2 energy, and see if the values converge with the number of grid points. Table 6.1 holds all the diagonal elements of the magnetizability and two first hypermagnetizability tensors for the water molecule. Figure 6.2 visualizes some aspects of this table. As is clear, the method converges rapidly with the number of weight points. Three points is not enough, but four or five provides good results for all but the highest order properties. If hypermagnetizabilities are needed, it may be reasonable to increase to as many as eight, but there is no purpose in going higher: improvements are negligible, and for 15 and 20 points, the quality is often reduced when compared with classical MP2. Häser observed that between 5 and 8 weight points were usually enough[26], which also fits experience with the LONDON implementation.

The reason why 15-20 weights in some cases reduce the quality of the results is probably because fitting a sum of exponentials is known to be a numerically delicate problem that easily leads to a near-singular system of equations.

6.2.6 Scaling

A naive example of linear scaling is counting the electrons in a chemical system – as the molecule increases, so does the computation time. This is a trivial case, and in this thesis, we will define linear scaling as a relationship of the form $t = an + b$ between computation time t and number of atoms n . The constant a represents how



(a) Hypermagnetizabilities in all directions.

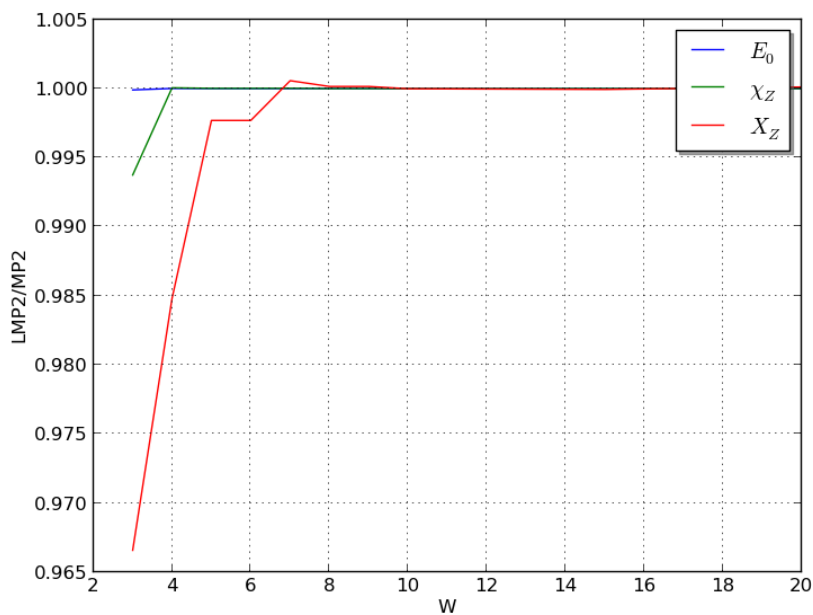
(b) Magnetic properties in z -direction.

Figure 6.2: Magnetic properties of water as a function of weight points. For each number of weights w , the found values are divided with the corresponding values found at the MP2 level. The y -axis is therefore dimensionless. The basis set is cc-pVDZ.

Table 6.1: The magnetic properties of H₂O calculated with classical MP2 and Laplace MP2, the latter with different number of weight points. Basis set is cc-pVDZ. The letter u refers to a Cartesian coordinate x, y, z .

Method, u	Weights	χ_{uu}	X_{uuuu}	X_{6u}
L-MP2, x	3.0	-2.882	77.911	-117728.432
	4.0	-2.731	3.172	2143.418
	5.0	-2.727	3.502	1855.036
	6.0	-2.727	3.502	1855.032
	7.0	-2.728	4.463	219.926
	8.0	-2.728	4.637	-0.218
	9.0	-2.728	4.637	-0.059
	10.0	-2.728	4.614	40.543
	15.0	-2.728	4.601	59.738
	20.0	-2.728	4.592	89.376
MP2, x	N/A	-2.728	4.595	69.554
L-MP2, y	3.0	-2.841	5.343	-101.319
	4.0	-2.802	2.677	798.322
	5.0	-2.800	2.694	790.554
	6.0	-2.800	2.694	790.552
	7.0	-2.800	2.714	782.013
	8.0	-2.800	2.720	780.285
	9.0	-2.800	2.720	780.338
	10.0	-2.800	2.719	780.866
	15.0	-2.800	2.718	781.386
	20.0	-2.800	2.714	799.919
MP2, y	N/A	-2.800	2.718	780.900
L-MP2, z	3.0	-2.793	9.139	1289.554
	4.0	-2.811	9.353	1855.827
	5.0	-2.811	9.478	1784.745
	6.0	-2.811	9.478	1784.738
	7.0	-2.811	9.505	1780.755
	8.0	-2.811	9.501	1778.264
	9.0	-2.811	9.501	1778.342
	10.0	-2.811	9.499	1779.272
	15.0	-2.811	9.501	1769.643
	20.0	-2.811	9.499	1786.654
MP2, z	N/A	-2.811	9.500	1778.841

computationally costly each basis function is and b indicates computation time that is spent regardless of basis functions like initialization and file handling.

The beauty of linear scaling is that even if it is infeasible to perform calculations on a certain system today due to lack of computational power, we can be certain that it will be doable in a few years – the famous Moore’s law states that the performance of a computer at a given price doubles every nine months, and this relationship has been remarkably stable over time. This implies that every seven and a half years, we can treat systems a thousand times larger. If a linearly scaling method can deal with small amino acids today, then the computers of tomorrow could perform equally accurate calculations on large bio molecules within a few years. Most methods

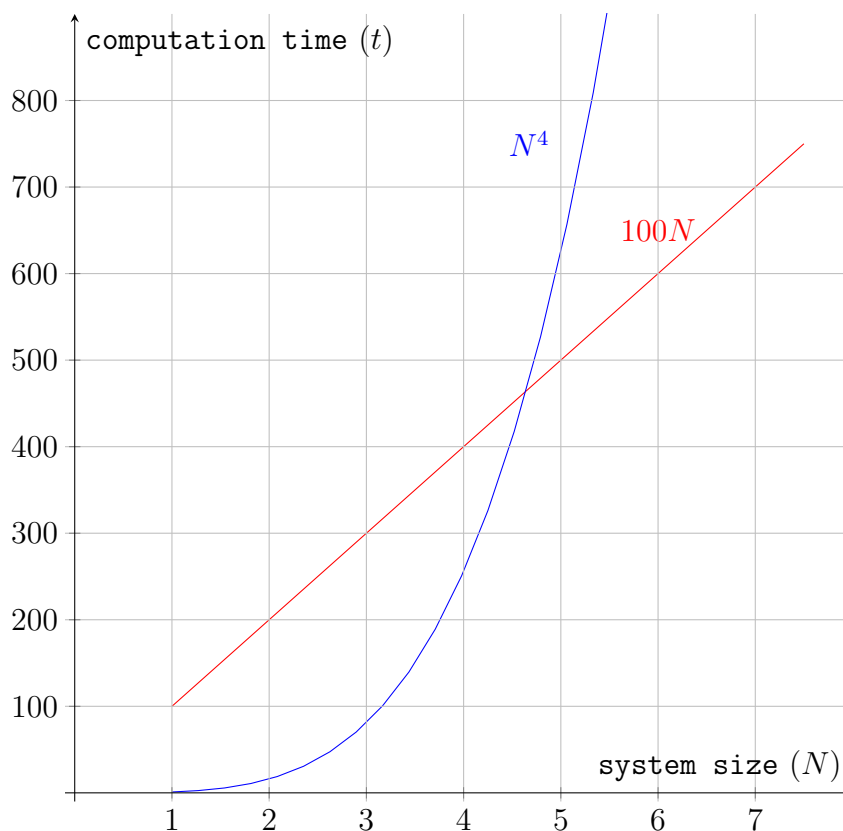


Figure 6.3: Plot of calculation time t as a function of system size N for various scaling regimes.

however, are *not* linearly scaling – double the number of atoms and the computation time typically increases as N^n where n is a number depending on the method in

question. Indeed, for Hartee-Fock, $n = 4$. The consequence of this is that as system size increases, computation time may soon exceed the age of the universe by several orders of magnitude, and then it is simply impossible to get results. This can be seen easily from figure 6.3. It is interesting to note that even if the linear scaling regime goes as $100N$, it will still be the best choice for a system five times larger than whatever is defined as 1 – at some point, the lines will cross. It also follows that even if linear scaling is unavailable, it will still be worth the effort to reduce the order of the problem; $100N^4$ is a lot better than N^5 if the system in question is big enough.

There is a difference between *formal scaling* and *typical scaling*. Formal scaling is the mathematically worst case scenario, but this often correspond to very peculiar molecular systems which are rarely or never encountered in practice. As such, the implemented variant of the Laplace-MP2 method could hypothetically scale as N^2 [26] in most cases or even linearly, provided integrals are properly screened [29].

Chapter 7

Results

The quality of the Laplace-MP2 method was tested and compared with regular MP2 theory for various systems. For smaller molecules, FCI was used for reasons of comparison, and for determining the reliability and quality of MP2 in magnetic fields. Most properties were calculated primarily with regular MP2 as it is faster than Laplace-MP2 in its present form. Several properties of small molecules were probed.

7.1 Molecules in magnetic fields

The behavior of some molecules in different magnetic fields was explored. He₂ received by far most attention, but also He₃ and BH were probed.

7.1.1 Helium clusters

In all situations, regardless of magnetic field, MP2 theory predicted a lower energy than HF theory, and slightly higher than FCI when that comparison was made. Also interesting to note is the bond distance and bond lengths as a function of magnetic field. This is seen in Table 7.1. When $\mathbf{B} = 0$, only dispersion forces are relevant, and HF theory does not detect any optimum distance, as expected. The MP2 and FCI methods do produce a very slight lowering of energy as the atoms are quite far apart. The MP2 calculation overestimates the optimum distance and underestimates the energy of this attraction, as it should: MP2 does not account for all of the correlation energy. The optimal bond length as predicted by MP2 becomes equivalent with FCI-geometry for magnetic fields slightly stronger than 1.5 a.u., and the HF-geometry improves steadily. This is clearly seen in figure 7.1. The HF calculations only account

Table 7.1: Bond length and bond energy of He₂ (oriented in the x -direction) as a function of magnetic field (varied in the z -direction) at the HF, MP2 and full CI theory levels. The basis set is aug-cc-pVTZ. B_z is magnetic field (a.u.), R is optimal distance between nuclei (bohr) and E^b is the bond energy (a.u.).

B_z	E_{HF}^b	R_{HF}	E_{MP2}^b	R_{MP2}	E_{CI}^b	R_{CI}
0.00	0.0	8.48	$1.77 \cdot 10^{-5}$	5.84	$2.66 \cdot 10^{-5}$	5.68
0.10	$5.70 \cdot 10^{-11}$	8.42	$2.06 \cdot 10^{-5}$	5.72	$3.08 \cdot 10^{-5}$	5.56
0.20	$7.49 \cdot 10^{-8}$	7.58	$3.24 \cdot 10^{-5}$	5.38	$4.73 \cdot 10^{-5}$	5.24
0.30	$5.50 \cdot 10^{-7}$	6.24	$5.71 \cdot 10^{-5}$	4.96	$8.06 \cdot 10^{-5}$	4.84
0.40	$3.59 \cdot 10^{-6}$	5.42	$1.03 \cdot 10^{-4}$	4.54	$1.40 \cdot 10^{-4}$	4.46
0.50	$1.35 \cdot 10^{-5}$	4.80	$1.77 \cdot 10^{-4}$	4.20	$2.32 \cdot 10^{-4}$	4.12
0.70	$6.15 \cdot 10^{-5}$	4.06	$4.15 \cdot 10^{-4}$	3.62	$5.22 \cdot 10^{-4}$	3.56
0.80	$9.90 \cdot 10^{-5}$	3.78	$5.85 \cdot 10^{-4}$	3.38	$7.26 \cdot 10^{-4}$	3.34
0.90	$1.51 \cdot 10^{-4}$	3.52	$7.98 \cdot 10^{-4}$	3.18	$9.76 \cdot 10^{-4}$	3.14
1.00	$2.23 \cdot 10^{-4}$	3.30	$1.06 \cdot 10^{-3}$	3.02	$1.28 \cdot 10^{-3}$	2.98
1.25	$4.99 \cdot 10^{-4}$	2.86	$1.90 \cdot 10^{-3}$	2.66	$2.23 \cdot 10^{-3}$	2.64
1.50	$9.50 \cdot 10^{-4}$	2.54	$3.02 \cdot 10^{-3}$	2.40	$3.47 \cdot 10^{-3}$	2.38
1.75	$1.72 \cdot 10^{-3}$	2.30	$4.54 \cdot 10^{-3}$	2.18	$5.09 \cdot 10^{-3}$	2.18
2.00	$2.94 \cdot 10^{-3}$	2.12	$6.53 \cdot 10^{-3}$	2.02	$7.19 \cdot 10^{-3}$	2.02
2.25	$4.61 \cdot 10^{-3}$	1.96	$8.93 \cdot 10^{-3}$	1.88	$9.69 \cdot 10^{-3}$	1.88
2.50	$6.67 \cdot 10^{-3}$	1.84	$1.17 \cdot 10^{-2}$	1.78	$1.25 \cdot 10^{-2}$	1.78
2.75	$9.13 \cdot 10^{-3}$	1.76	$1.48 \cdot 10^{-2}$	1.70	$1.57 \cdot 10^{-2}$	1.70

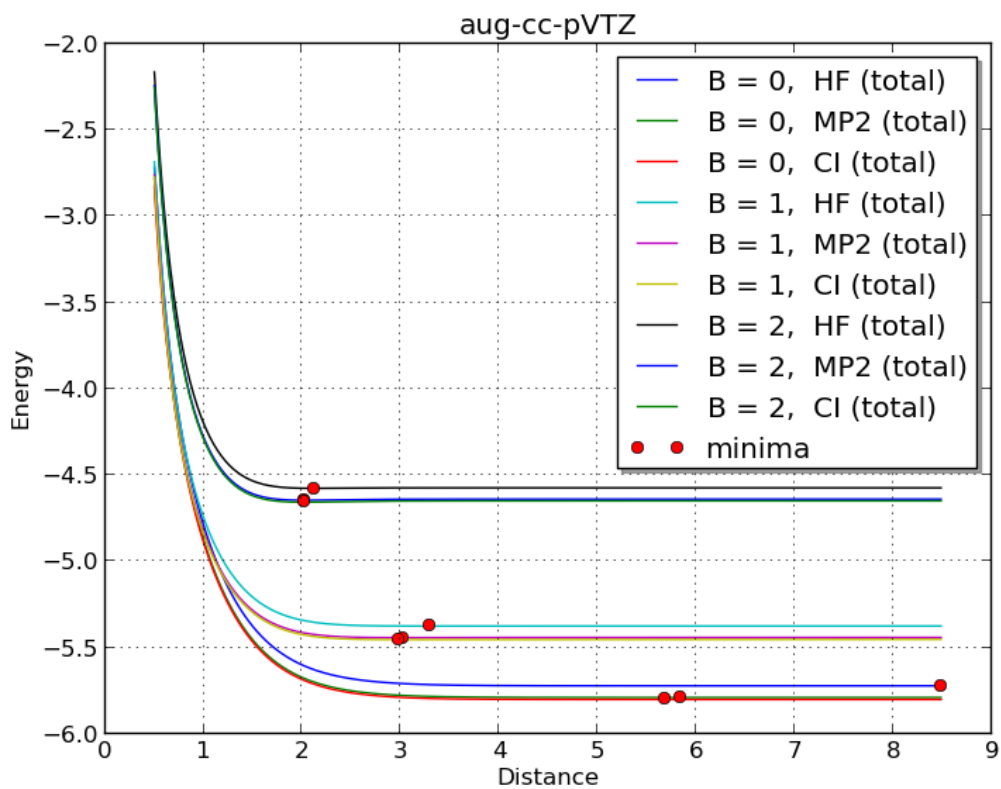


Figure 7.1: Dissociation curves for He₂ calculated at three different theory levels (HF, MP2 and FCI) and at three different magnetic fields orthogonal to the molecular axis. Energy are in atomic units, distances in bohr. The basis set is aug-cc-pVTZ.

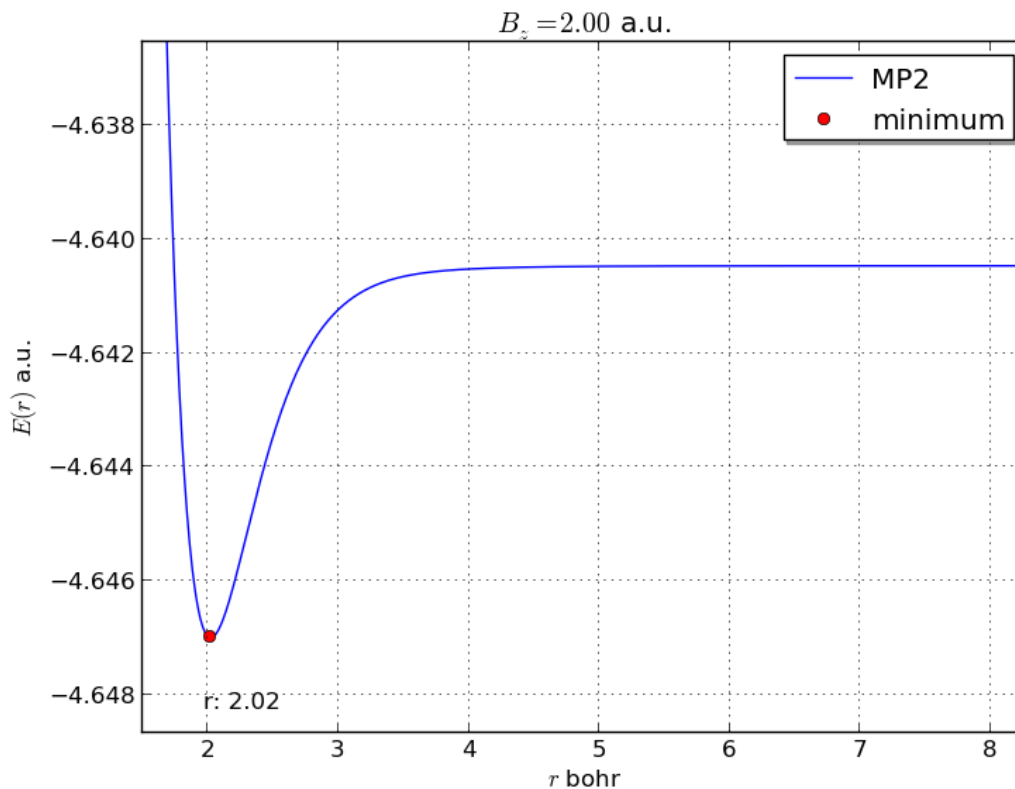


Figure 7.2: Dissociation curve calculated at the MP2 level for He_2 at $B_z = 2$ a.u. The basis set is aug-cc-pVTZ.

Table 7.2: Bond length and bond energy of He_2 (oriented in the x -direction) as a function of magnetic field (varied in the z -direction) at the HF, MP2 and FCI theory levels. The basis set is aug-cc-pVTZ. B_z is the the magnetic field (a.u.), R is the optimal distance between nuclei (bohr) and E^t is the total energy of the molecule.

B_z	R_{HF}	E_{HF}^t	R_{MP2}	E_{MP2}^t	R_{CI}	E_{CI}^t
0.0	8.48	-5.72244546	5.84	-5.79009657	5.68	-5.8017051
1.0	3.30	-5.37597054	3.02	-5.44336931	2.98	-5.45438541
2.0	2.12	-4.57770328	2.02	-4.64699537	2.02	-4.65775641

for about half of the bond energy. In other words, the HF method may produce a decent estimate of the molecular structure in strong magnetic fields, but it will underestimate the bond strength. MP2 on the other hand, predicts a bond strength that rapidly converges with FCI. All methods are in better agreement for both bond length and bond energy as the field increases. It must be stressed that these bonds are very weak and that Figure 7.2 shows a selected cut of the dissociation curve at $B_z = 2$ a.u.

Dependence on orientation

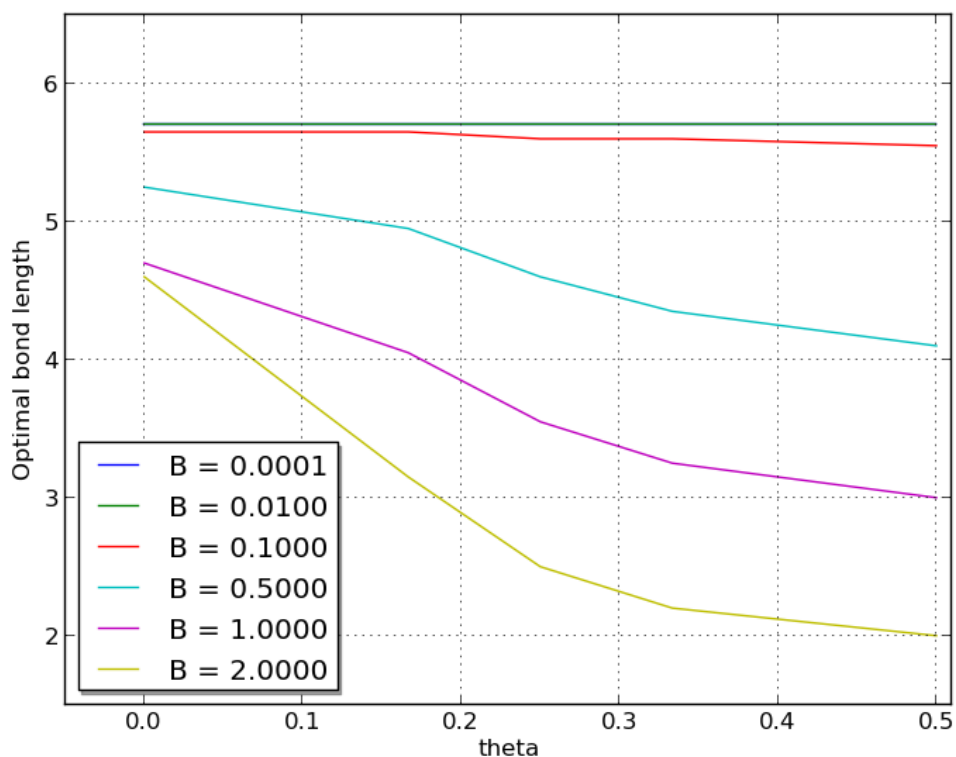


Figure 7.3: Optimal bond length for He_2 as a function of the angle of the magnetic field. The angle θ was varied from 0 to $\frac{\pi}{2}$ relative to the molecular axis, and the total size of the field varied from 10^{-4} a.u. to 2 a.u. The x -axis is the orientation of the field, the y -axis is the optimum bond length in bohr. The basis set is aug-cc-pVTZ.

Figure 7.3 shows how the optimal geometry of He_2 changes as a function of magnetic field strength and orientation to the molecular axis. For weak fields, the orientation is irrelevant, which is hardly surprising. As the field increases, the molecule is invariably compressed, but much less so if the field is parallel to the molecular axis.

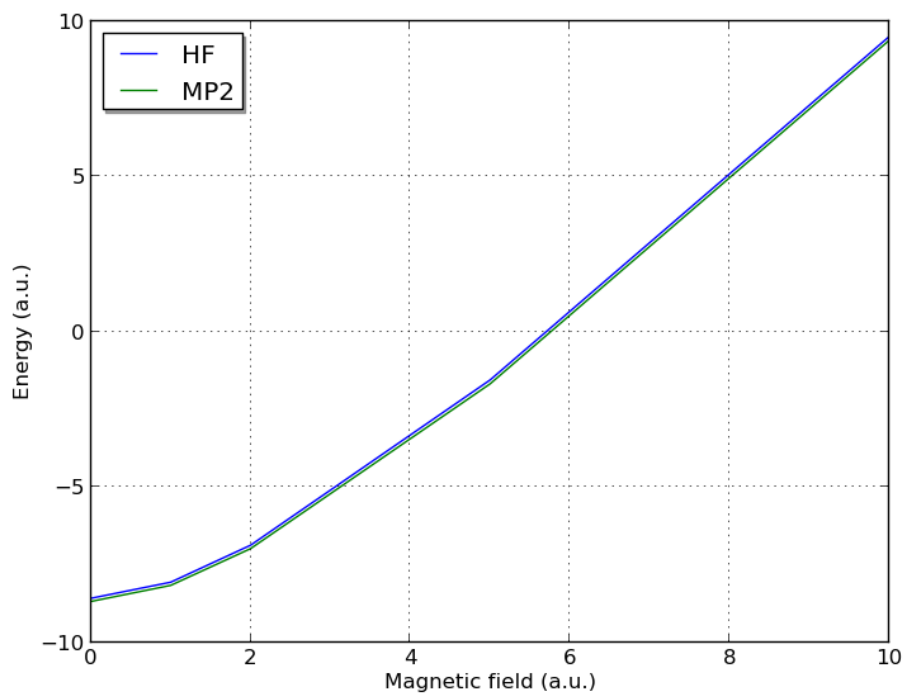
Helium trimers

The trimer of helium was also explored. Previous research indicates that clusters of helium atoms in magnetic fields will assume a planar grid of nearly equilateral triangles orthogonal to the field [30]. To simplify calculations, all He_3 molecules were given the shape of such a regular polygon in the xy -plane, and the field varied in the z -direction. The total energy of the system increased with the magnetic field, but the size of the triangle decreased consistently. These two trends are seen in figures 7.4a and 7.4b respectively. The distance between the lines in the latter figure is nearly uniform for the entire interval, indicating that HF produces systematic errors. One interesting thing to note is that HF and MP2 calculations corresponds better as the magnetic fields increases: for zero field, MP2 predicts a much shorter optimal distance than HF. This is not surprising by itself, since the only attraction at zero field is dispersion, and HF theory does not pick this up at all¹ in contrast to MP2 theory. The “bump” of the graph is of course extremely small. As the magnetic field gets stronger, the difference in predicted geometry disappears, and both HF and MP2 produces the exact same optimal paramagnetic bond length at 10a.u. These calculations would cause the SCF-routine in LONDON to fail to converge for larger distances.

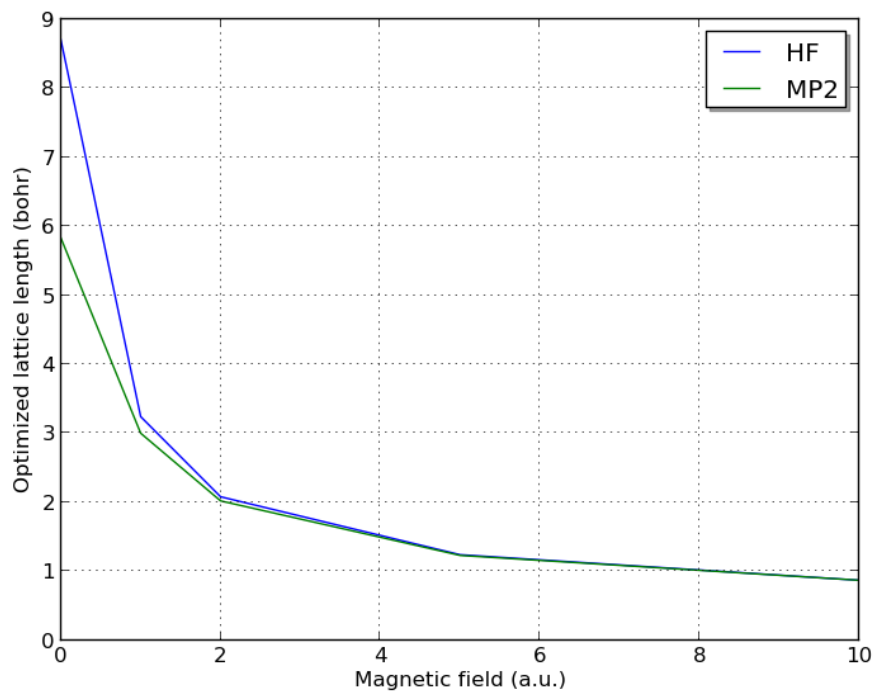
7.1.2 An example of paramagnetic stabilization

The boron monohydride molecule (BH) was briefly scanned using a pre-optimized bond length of 2.3342 and perpendicular fields of increasing size. As is seen in Figure 7.5a, both the HF and MP2 calculations predict a significant minimum energy for magnetic fields in the vicinity of 0.23 a.u. This is an example of paramagnetic stabilization, and agrees well with previous estimates [31]. The MP2 contribution to the energy is interesting, however: it is always negative, thus lowering the total energy as expected. But, the difference between the HF and MP2 estimates is largest at the two extremes. In effect, the MP2 contribution modifies the HF estimate of the influence of the field, making the lowest energy be found for a slightly stronger field at the MP2 level. The MP2 contribution is least negative at $B_z = 0.1355$ a.u. It should

¹The fact that it seemingly does could be caused by basis set superposition.

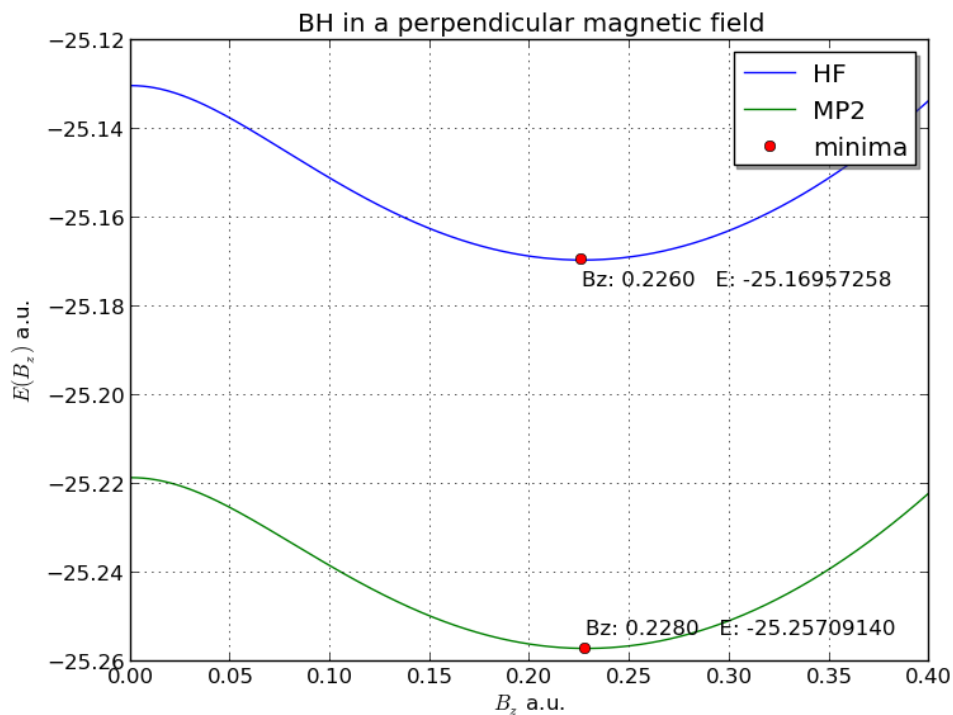


(a) Total energy as a function of magnetic field strength.

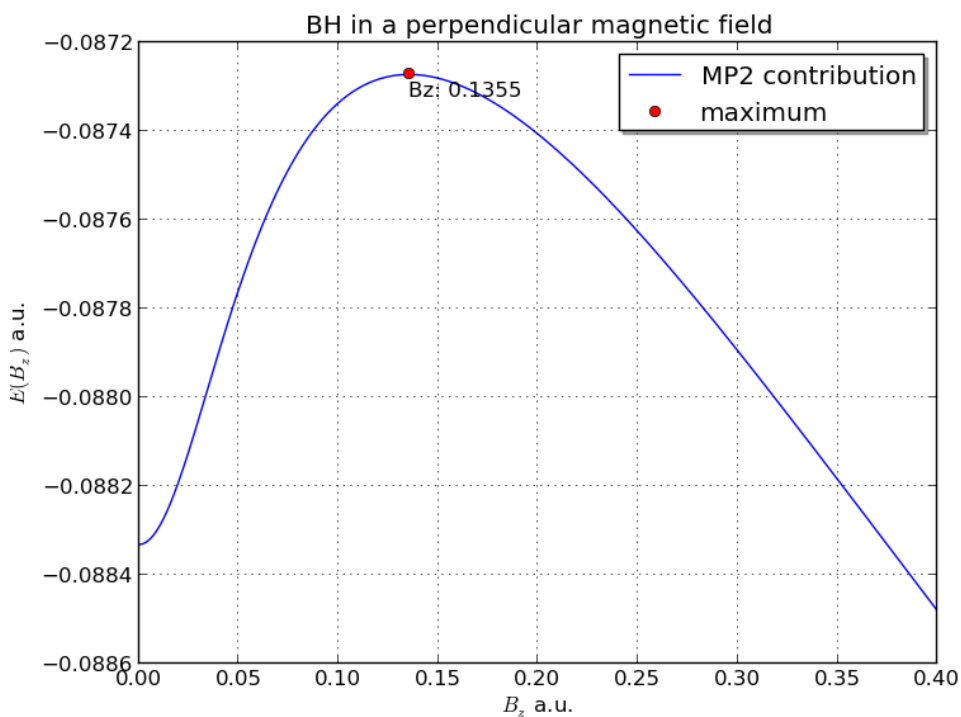


(b) Lattice length with lowest energy as a function of magnetic field strength.

Figure 7.4: The shape of the equilateral triangles and their energy depends on the strength of the magnetic field.



(a) MP2 and HF total energy.



(b) MP2 contribution to energy

Figure 7.5: BH in a perpendicular field. The basis set is aug-cc-pVTZ.

be noted that the difference between the largest and smallest MP2 contribution in this data set is only $1.2 \cdot 10^{-3}$ a.u. The MP2 corrections in this case has little effect on relative energies.

7.2 Magnetizabilities and hypermagnetizabilities

Magnetizabilities and hypermagnetizabilities were calculated for some small molecules. Table 7.3 shows results for H₂O and He₂. We see immediately that the method is consistent; regardless of the orientation of the magnetic field, E_0 does not change. Also, in the case of the dimer (which is aligned at the x -axis, all values are identical for a field lying in y - or z -direction. All the diagonal elements of χ are negative for both molecules. For H₂O this corresponds with observations: water is diamagnetic. He₂ has obviously not been probed experimentally. Table 7.4 holds data for H₂O and HF as calculated with decontracted basis sets at HF and MP2 levels. The molecular geometry of water was identical to those used in the article by Tellgren *et al.* [32] and is seen in section A.1.2. The geometry of the HF molecule was manually optimized, and is therefore slightly different. For the water molecule, all values at the HF level are identical to those in the article. For hydrogen fluorine, where the bond length is slightly different, all values except the hypermagnetizabilities perpendicular to the molecular axis are identical as well.

Table 7.4 also shows how important correlation energy is for higher order trends: for both HF and H₂O, E_0 differs by about 0.5%. The values of χ differs with 3% and the discrepancies between the HF and MP2 estimates of the hypermagnetizabilities are sometimes as large as 70%.

Table 7.3: The magnetic properties in three directions of H₂O and He₂, calculated with MP2. The basis set is aug-cc-pVTZ. ($u \in [x, y, z]$)

Molecule	Orientation	E_0	χ_{uu}	X_{uuuu}	X_{6u}
H ₂ O	x	-76.381991	-3.041863	25.881052	781.946641
	y	-76.381991	-2.996323	18.736066	-1248.301506
	z	-76.381991	-3.041540	16.684437	751.719729
He ₂	x	-5.790096	-0.794617	1.935470	-52.175107
	y	-5.790096	-0.794045	1.976424	-172.552017
	z	-5.790096	-0.794045	1.976424	-172.552017

Table 7.4: Magnetic properties of water and hydrogen fluoride at the HF and MP2 level. The HF-values agrees with previous publications [32]. Basis set is decontracted aug-cc-pVTZ. The hydrogen fluoride molecule is aligned in the z -direction and the bond length is 1.739 bohr.

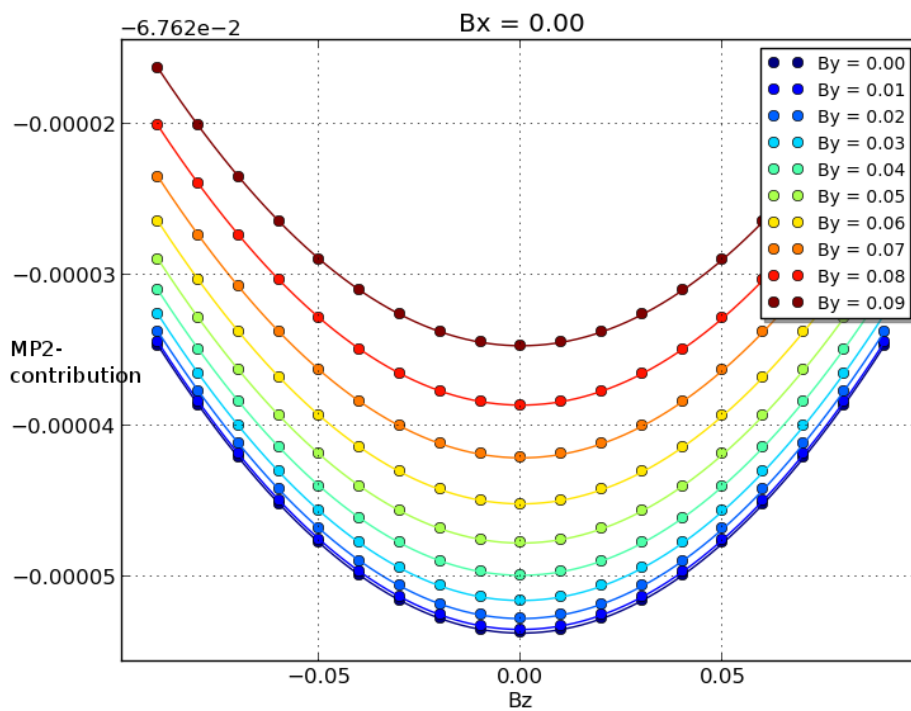
Molecule	Method	E_0	χ_{xx}	χ_{yy}	χ_{zz}	X_{xxxx}	X_{yyyy}	X_{zzzz}
H ₂ O	Hartree-Fock	-76.062	-2.953	-2.899	-2.942	22.424	14.949	12.873
	MP2	-76.382	-3.042	-2.996	-3.042	18.736	25.881	16.684
HF	Hartree-Fock	-100.062	-2.228	-2.228	-2.117	8.022	8.022	5.814
	MP2	-100.398	-2.303	-2.303	-2.192	9.870	9.871	7.678

7.2.1 Magnetic properties of He₂

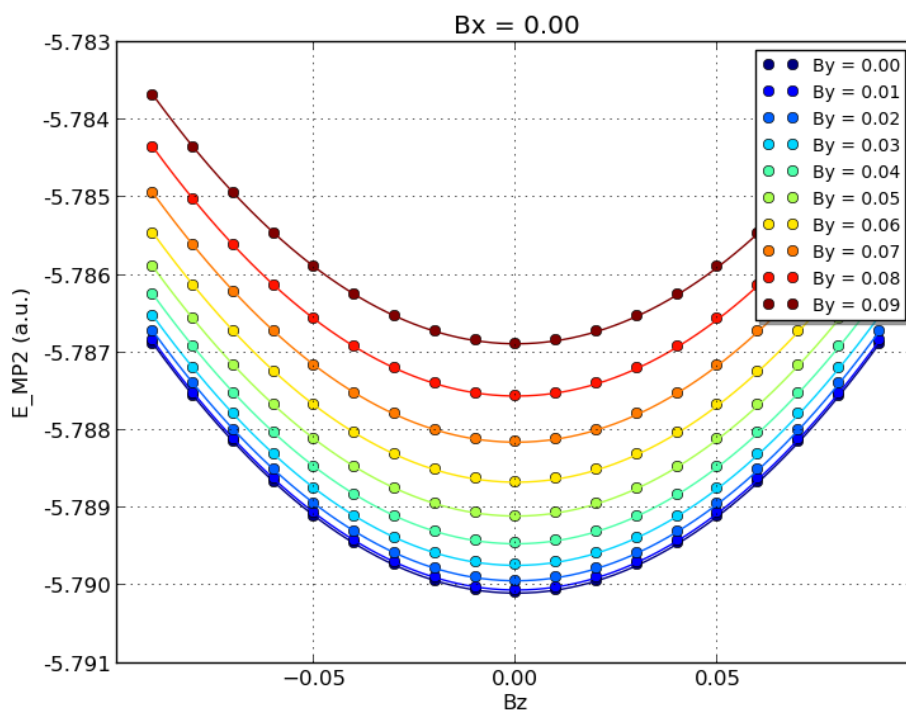
Since the magnetic properties are defined by a Taylor expansion around $\mathbf{B} = 0$ and the properties at equilibrium are most relevant, He₂ was geometrically optimized with MP2 and FCI with the aug-cc-pVTZ basis set. The energetically optimum distance was found to be 5.68 bohr at the FCI level, a geometry used for all following explorations. The magnetic field was systematically varied along the Cartesian axis with ten points in the interval 0.00 a.u. to 0.09 a.u. Figure 7.6 shows how the MP2 correlation energy and the MP2 total energy behave as a function the magnetic field. The magnetic field is held to be 0 in the x -axis. Figure 7.6b is not very surprising: as the magnetic field increases, so does the total energy. However, figure 7.6a shows how the correlation energy varies with the magnetic field. For one thing, we get the same profile that can be excellently approximated by a second order polynomial. The HF energy already behaves this way (and is by far dominant). So, the correlation energy serves to slightly increase the effects we see; namely that the total energy of the system rises with the magnetic field.

7.2.2 Magnetic properties of water

The magnetizabilities and hypermagnetizabilities of water were also calculated. In these cases, the molecular geometry seen in section A.1.1 was used. As Figure 7.7a shows, the energy of water increase with the magnetic field, and the term is negative, serving to place the total energy lower than the HF energy. Still, this difference is small.

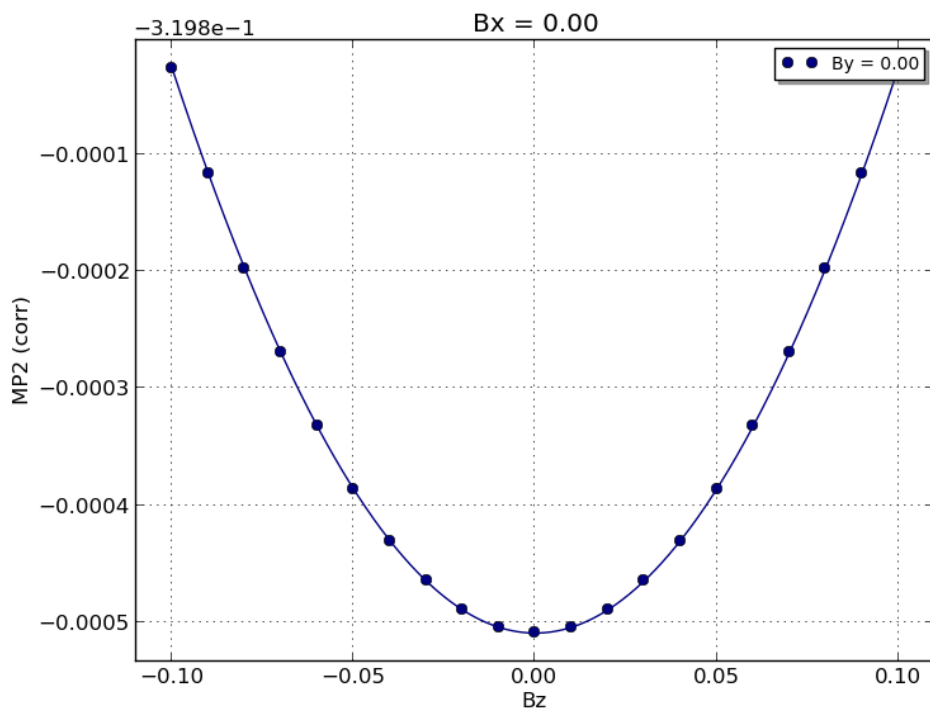


(a) MP2 contribution (a.u.)

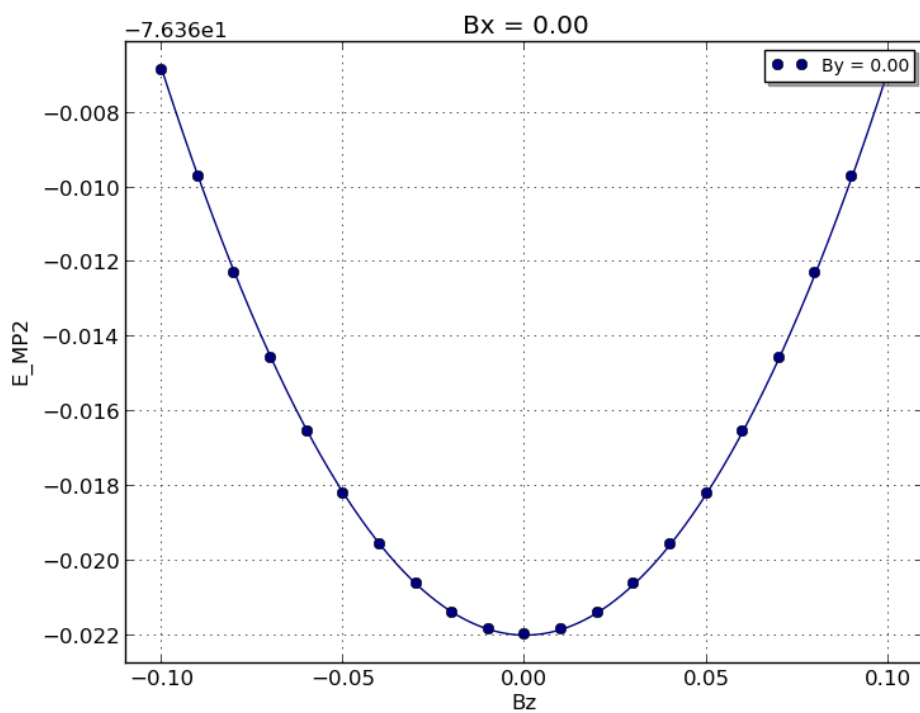


(b) MP2 total energy.

Figure 7.6: The energy and MP2 contribution as a function of magnetic field for He_2 . The molecule is parallel to the x-axis, and B-field in x-direction is 0.



(a) MP2 correlation energy.



(b) MP2 total energy.

Figure 7.7: $E(\mathbf{B})$ for H_2O , MP2 contribution and MP2 total energy of water. The \mathbf{B} -field in x - and y -direction is 0. Basis set is aug-cc-pVTZ.

7.2.3 London orbitals and basis set convergence

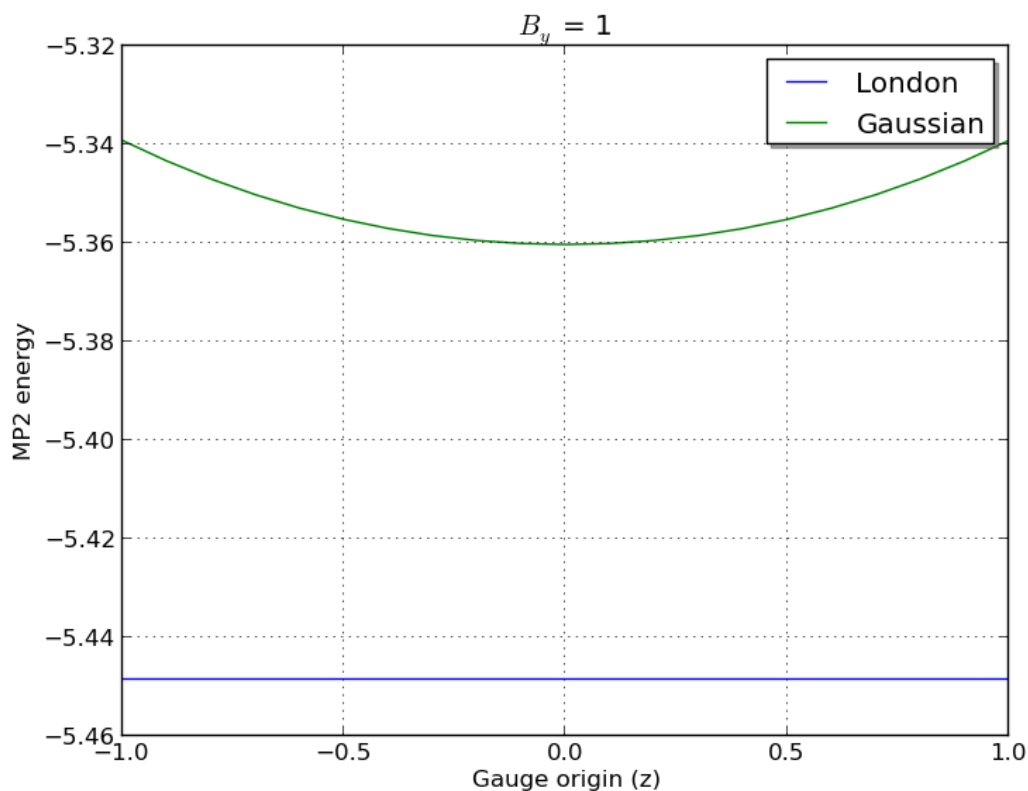


Figure 7.8: MP2 total energy of He_2 as a function of gauge origin. The molecule is oriented along the x -axis, with each atom at 2.84 bohr from origo. Therefore, the electronic center is at the Cartesian center. The magnetic field was set to 1.0 a.u. along the y -axis, and the gauge-origion was varied in the z -direction. The basis set is aug-cc-pVQZ

The importance of the gauge origin invariance has been briefly explored. First, the effects of the gauge-origin was explored, as seen in Figure 7.8. The LGTOs produce the same result regardless of the position of the gauge origin, and provides a lower estimate of energy in all cases. GTOs does not include the gauge origin, and the results gets gradually worse as it is moved from the electronic center of the molecule. The error is symmetric, which matches the symmetric nature of the molecule. Table 7.5 shows magnetic properties calculated with different basis sets. As expected, E_0

Table 7.5: Magnetic properties of He₂ calculated with different basis sets, with and without the London-factor.

Orbital type	basis set	E_0	χ_{yy}	X_{yyyy}
GTO	6-31G	-5.73272023	-8.84518347	0.51378280
	6-311G	-5.74559493	-8.85802672	0.94526240
	cc-pVDZ	-5.76198308	-4.23452672	18.20072371
	cc-pVTZ	-5.78888261	-2.40420539	24.59658956
	aug-cc-pVTZ	-5.79009576	-0.86640656	-8.83870848
	aug-cc-pVQZ	-5.79498075	-0.81182282	-3.00327551
LGTO	6-31G	-5.73272023	-0.77969875	0.52411332
	6-311G	-5.74559493	-0.79256658	0.97308743
	cc-pVDZ	-5.76198308	-0.77819428	0.51563609
	cc-pVTZ	-5.78888261	-0.79000889	1.24848925
	aug-cc-pVTZ	-5.79009576	-0.79404334	1.97094529
	aug-cc-pVQZ	-5.79498075	-0.79236025	1.94556773

is not affected by choice of orbital type, and the calculated energy decreases as the size of the basis increases. This is typical for all methods, even the non-variational variants. Calculating magnetizabilities with GTOs requires large basis sets in order to approximate similar calculations with LGTOs, but the convergence is evident – the differences between LGTOs and GTOs decrease as bigger basis sets are used. The difference between the lowest and highest estimate is about one hundred times larger for the GTO based calculations. For the hypermagnetizabilities, GTO based calculations do not appear to converge at all. With the London factor included, hypermagnetizabilities calculated with the smallest and largest basis sets have the same sign, and vary by less than a factor 20. In other words, a small basis and LGTOs provide a reliable estimate of what larger basis sets will reproduce. GTOs do not.

7.2.4 Order of polynomial fitting

Table 7.6 shows how the calculated values converge as the order of the polynomial used for fitting the data points increase. As long as there are enough data points to use a higher order polynomial, this is an advantage: one can get higher order values,

Table 7.6: Magnetic properties and their dependency on the order of the polynomial used to fit the data.

Molecule	Order	E_0	χ_{uu}	X_{uuuu}	X_{6u}	X_{8u}
H ₂ O	2	-76.381983	-2.982008			
	4	-76.381991	-2.996141	18.125155		
	6	-76.381991	-2.996323	18.736066	-1248.301506	
	8	-76.381991	-2.996328	18.768817	-1410.359583	460827
He ₂	2	-5.79497995	-0.79086871			
	4	-5.79498075	-0.79234445	1.89255574		
	6	-5.79498075	-0.79236025	1.94556773	-108.32170260	
	8	-5.79498075	-0.79236205	1.95690449	-164.41841189	159517

and the quality of lower order values seems to increase. Convergence is very fast, so it is probably enough to use a polynomial one degree higher than the highest order term needed. This table contains more decimals than the quality of the methods used (MP2 and polynomial fitting) can justify, so these values should not be taken to be exact for this number of digits. The extra digits are simply included since the trends would not be visible otherwise – the polynomial fitting is a numerically stable approach, and the values of lower order properties are affected less and less as additional terms are included.

7.2.5 An example of MP2 failing

For all quantum mechanical methods, it is important to know what the method can do, what it cannot do, how consistent it is and what systems it cannot reliably describe. The main purpose of introducing MP2, as per the discussion in section 1.2 is to enable calculation of electron correlation for larger systems. Therefore, it is important to know how the MP2 contribution compares with the FCI contribution. Table 7.7 shows a comparison. The optimum bond length at zero field is 5.68 bohr, while at a perpendicular field of 1a.u., it is about 2.98 bohr. MP2 consistently reproduces between 80% and 87% of the correlation energy, except when the atoms are very close. It should be noted that when the atoms in a He₂ molecule are very close, the entire specimen will electronically start to resemble a beryllium atom. In this case ($\mathbf{B} = 0$), we go from two atoms in the $1s^2$ configuration to one atom

Table 7.7: The correlation energy of He_2 at the MP2 and CI theory level and the quotient between them at different magnetic fields and at two different geometries. Basis set is aug-cc-pVTZ.

Bond length	$B(\mathbf{z})$	E_{MP2}	E_{CI}	$\frac{E_{\text{MP2}}}{E_{\text{CI}}} \times 100\%$
0.50	0.0	-0.06294907	-0.11190677	56.25
	0.1	-0.06936125	-0.11895458	58.30
	0.2	-0.06868727	-0.08444630	81.33
	0.3	-0.07048593	-0.08535466	82.58
	0.4	-0.07193852	-0.08633541	83.32
	0.5	-0.07304683	-0.08691569	84.04
	0.6	-0.07393125	-0.08727561	84.71
	0.7	-0.07467418	-0.08755163	85.29
	0.8	-0.07531498	-0.08779496	85.78
	0.9	-0.07586539	-0.08800778	86.20
	1.0	-0.07632837	-0.08818009	86.55
5.68	0.0	-0.06767372	-0.07928305	85.35
	0.1	-0.06765035	-0.07924431	85.36
	0.2	-0.06758480	-0.07913506	85.40
	0.3	-0.06748527	-0.07896806	85.45
	0.4	-0.06736330	-0.07876122	85.52
	0.5	-0.06722925	-0.07853143	85.60
	0.6	-0.06709100	-0.07829198	85.69
	0.7	-0.06695442	-0.07805257	85.78
	0.8	-0.06682327	-0.07781965	85.86
	0.9	-0.06669963	-0.07759729	85.95
	1.0	-0.06658401	-0.07738715	86.04

with $1s^22s^2$. However, the $2p$ orbital is very close in energy, and so we get nearly degenerate states. This indicates the presence of static correlation, and so MP2 is no longer adequate for describing the system. When the field is increased, the orbital Zeeman term is sufficiently large to force the $2p_{-1}$ orbital to have lower energy than $2s$, and the degeneracy disappears.

Part IV
Discussion

Chapter 8

Conclusion

8.1 About the implementation

A regular MO-based MP2 algorithm and an AO-based, Laplace transform variant was successfully introduced to the LONDON program. Both methods can successfully reproduce known results, and can reliably be used to perform quantum chemical calculations with or without finite magnetic fields. Even more, the combination of MP2 theory and LGTOs can be used to explore properties that at present are not accessible by any other means.

8.1.1 MP2 in the CAS-type methods

The MP2-solver implemented in the CAS-CI and CAS-SCF modules has been completed. It is fairly well optimized as it is, and further optimization is unnecessary – CAS-type calculations are invariably much more time consuming than MP2, so the time spent on determining the MP2 contribution is negligible in comparison. This is likewise true for the free-standing module of the same implementation.

8.1.2 Laplace MP2

The L-MP2 method is to date a pilot implementation, and several improvements can be made. L-MP2 only accepts a RHF starting point, but UHF and GHF can (and will) be implemented in the future. Integral screening is missing, and the L-MP2 method is only competitive with this in place. Also, there are many possible optimizations that can be implemented with the potential to drastically reduce execution speed. Most of this work is about replacing the brute-force multiply nested

loops in the transformation routines with the built-in tensor functionality and Lapack routines. This kind of work is time consuming and error prone, and so a working prototype of the method was deemed more relevant than a fully optimized solver, at least initially. However, the ambition is to be able to use LONDON for more involved calculations, and for that to happen, such improvements are required. Especially since the program is not optimized primarily for speed, it is vitally important to save some computational resources wherever possible.

This, in turn, may open up for calculations at the MP2-level on molecular systems hitherto impossible, especially in strong magnetic fields. Molecules in strong magnetic fields is a largely unexplored area of quantum chemistry, and gauge invariant implementations of MP2 have not been done until now. Laplace-MP2 has been implemented elsewhere by others [33, 27, 34], but it is not a commonly encountered method.

Another feature that is missing is parallelization. The memory consumption of a calculation can be tailored because of the basis set splitting, and so parallelization can be exploited very efficiently. Also, since a calculation for each weight point can be run independently of the algorithm could possibly be performed on a distributed level.

8.2 Discussion of the results

MP2 theory consistently produces energy estimates that are lower than those predicted at the HF level, and slightly higher than those computed with FCI theory. The MP2 method does not exhibit any aberrant behavior in weak or strong magnetic fields. It must be emphasized that none of the systems probed in this thesis are known to cause trouble at the MP2 theory level. A dissociation of H_2 for example, would certainly cause an MP2 calculation to diverge. Helium clusters, on the other hand, constitutes “nice” systems, as dispersion are important and MP2 theory is known to handle dispersion very well.

When helium nuclei are very close, MP2 theory is significantly outperformed by FCI calculations. This is expected, since MP2 theory cannot handle static correlation.

One of the most interesting results was that the MP2 contribution changes very little with the magnetic field. This implies that while HF theory overestimates the energy, it is fairly systematic and consistent and the errors produced are largely independent of the magnetic field.

8.2.1 Geometrical properties

A magnetic field usually raises the total energy of a system. If strong enough, it can cause otherwise anti-bonding specimens to occur. MP2 can be used to accurately predict these bond lengths, especially as the strength of the field increases. The MP2 method outperforms the HF method at all tested magnetic fields for geometry optimizations. HF theory produces bonds that are too weak and too long, even at strong magnetic fields. The MP2 method on the other hand, underestimates the bond strength (thus overestimating bond length) for weak fields, but much less so than the HF counterpart. For strong fields, it is in excellent agreement with calculations performed at the FCI level. In the absence of magnetic fields, MP2 is known to produce good estimates for most molecular geometries. It appears to do equally well in the more general case.

8.2.2 Magnetic properties

Magnetizabilities and hypermagnetizabilities have not been calculated at the MP2 level until now. When compared with values at the Hartree-Fock level, MP2 in general apparently provides estimates of the magnetizabilities that are quite similar, whereas the values for hypermagnetizabilities can be quite different. This implies that correlation is not the most important contribution to these magnetic properties, but that it should not be neglected, especially for higher order properties as per the observations in section 7.2.

8.2.3 Future systems to be explored

The most immediately desirable purpose of the Laplace-MP2 method is to use it to perform calculations on as large molecules as possible. We know very little about how moderate to large molecules behave in strong magnetic fields, since the only available *ab initio* method that can handle such systems is HF, which does not include correlation.

Bibliography

- [1] John Bannister Goodenough. *Magnetism and the Chemical Bond*. Wiley, first edition, 1963.
- [2] Jürgen Gauss. Effects of electron correlation in the calculation of nuclear magnetic resonance chemical shifts. *J. Chem. Phys.*, 99(5):3629–3643, 1993.
- [3] R. Ditchfield. Theoretical studies of magnetic shielding in H_2O and $(\text{H}_2\text{O})_2$. *J. Chem. Phys.*, 65(8):3123–3133, 1976.
- [4] Erik I. Tellgren. *Quantum-chemical method developement for extended and magnetic systems*. PhD thesis, University of Oslo, 2009.
- [5] David J. Griffiths. *Introduction to Quantum Mechanics*. Pearson, first edition, 2005.
- [6] P. Atkins and R. Friedman. *Molecular Quantum Mechanics*. Oxford University Press, fourth edition, 2008.
- [7] Trygve Ulf Helgaker, Poul Jørgensen, and Jeppe Olsen. *Electronic Structure Theory*. Wiley, first edition, 2000.
- [8] Jun John Sakurai. *Modern Quantum Mechanics*. Addison-Wesley Publishing Company, 1994.
- [9] Trygve Helgaker and Poul Jørgensen. An electronic hamiltonian for origin independent calculations of magnetic properties. *J. Chem. Phys.*, 95(4):2595–2601, 1991.
- [10] U. Kappes and P. Schmelcher. Atomic orbital basis set optimization for ab initio calculations of molecules with hydrogen atoms in strong magnetic fields. *J. Chem. Phys.*, 100(4):2878–2887, 1994.

- [11] Kai K. Lange, Erik I. Tellgren, M. R. Hoffmann, and Trygve U. Helgaker. A paramagnetic bonding mechanism for diatomics in strong magnetic fields. *Science*, 337:327–331, 2012.
- [12] Patrick M. Colletti. Size "h" oxygen cylinder: Accidental mr projectile at 1.5 tesla. *Journal of Magnetic Resonance Imaging*, 19:141–143, 2004.
- [13] B. A. Boyko, A. I. Bykov, M. I. Dolotenko, N. P. Kolokolchikov, I. M. Markevtsev, O. M. Tatsenko, and K. Shuvalov. With record magnetic fields to the 21st Century. *Pulsed Power Conference, 1999. Digest of Technical Papers. 12th IEEE International*, 2:746–749, 1999.
- [14] Detlev Koester and Ganesar Chanmugam. Physics of white dwarf stars. *Rep. Prog. Phys.*, 53:837–915, 1990.
- [15] R H Garstang. Atoms in high magnetic fields (white dwarfs). *Rep. Prog. Phys.*, 40(2):105–154, 1977.
- [16] Michael Victor Berry and Andre Konstantin Geim. Of flying frogs and levitrons. *European Journal of Physics*, 18:307–313, 1997.
- [17] G. I. Pagola, M. C. Caputo, M. B. Ferraro, and P. Lazzeretti. Calculation of the fourth-rank molecular hypermagnetizability of some small molecules. *J. Chem. Phys.*, 120(20):9556–9560, 2004.
- [18] Fritz London. Théorie quantique des courants interatomiques dans les combinaisons aromatiques. *J. Phys. Radium*, 8(10):397–409, 1937.
- [19] C.J. Cramer. *Essentials of Computational Chemistry: Theories and Models*. John Wiley & Sons, second edition, 2004.
- [20] Jos. M. Thijssen. *Computational Physics*. Cambridge University Press, second edition, 2007.
- [21] Sharon Hammes-Schiffer and Hans C. Andersen. The advantages of the general hartree-fock computer simulation of materials method for future. *J. Chem. Phys.*, 99:1901–1913, 1993.
- [22] Isaiah Shavitt and Rodney J. Bartlett. *Many-Body Methods in Chemistry and Physics*. Cambridge University Press, first edition, 2009.
- [23] F. Jensen. *Introduction to Computational Chemistry*. John Wiley & Sons, second edition, 2007.

- [24] A. Szabo and N.S. Ostlund. *Modern Quantum Chemistry: Introduction to Advanced Electronic Structure Theory*. Dover Books on Chemistry Series. Dover Publications, 1996.
- [25] Jan Almlöf. Elimination of energy denominators in Møller–Plesset perturbation-theory by a Laplace transform approach. *Chem. Phys. Lett.*, 181(4):319–320, 1991.
- [26] Marco Häser. Møller-plesset (mp2) perturbation theory for large molecules. *Theor Chim Acta*, 87:147–173, 1993.
- [27] Bernd Doser, Jan Zienau, Lucien Clin, Daniel S. Lambrecht, and Christian Ochsenfeld. A linear-scaling MP2 method for large molecules by rigorous integral-screening criteria. *Z. Phys. Chem.*, 224(3-4):397–412, 2010.
- [28] Simon A. Maurer, Daniel S. Lambrecht, Jörg Kussmann, and Christian Ochsenfeld. Efficient distance-including integral screening in linear-scaling Møller–Plesset perturbation theory. *J. Chem. Phys.*, 138(1):014101, 2013.
- [29] Bernd Doser, Daniel S. Lambrecht, and Christian Ochsenfeld. Tighter multipole-based integral estimates and parallel implementation of linear-scaling ao-mp2 theory. *Phys. Chem. Chem. Phys.*, 10:3335–3344, 2008.
- [30] Erik I. Tellgren, Simen Sommerfelt Reine, and Trygve Helgaker. Analytical GIAO and hybrid-basis integral derivatives: application to geometry optimization of molecules in strong magnetic fields. *Phys. Chem. Chem. Phys.*, 14(26):9492–9499, 2012.
- [31] Erik I. Tellgren, Trygve Helgaker, and Alessandro Soncini. Non-perturbative magnetic phenomena in closed-shell paramagnetic molecules. *Phys. Chem. Chem. Phys.*, 11(26):5489–5498, 2009.
- [32] Erik I. Tellgren, Alessandro Soncini, and Trygve Helgaker. Nonperturbative ab initio calculations in strong magnetic fields using london orbitals. *J. Chem. Phys.*, 129, 2008.
- [33] Bernd Doser, Daniel S. Lambrecht, Jörg Kussmann, and Christian Ochsenfeld. Linear-scaling atomic orbital-based second-order Møller–Plesset perturbation theory by rigorous integral screening criteria. *J. Chem. Phys.*, 130(6):064107, 2009.

- [34] Marco Häser and Jan Almlöf. Laplace transform techniques in Møller–Plesset perturbation theory. *J. Chem. Phys.*, 96(1):489–494, 1992.

Part V
Appendix

Appendix A

Input data

A.1 Molecular geometries

A.1.1 Water

This geometry was used for most calculations performed on the water molecule.

O	0.00	-0.188	0.00
H	1.42	0.881	0.00
H	-1.42	0.881	0.00

A.1.2 Water II

This geometry was used in Tellgren et. al.'s article of 2008 [32].

O	0.0	0.0	0.124144424
H	0.0	1.43153	-0.985265576
H	0.0	-1.43153	-0.985265576